

YITP-06-29 KEK-TH-1091 hep-ph/0607255

Physics potential of T2KK: An extension of the T2K neutrino oscillation experiment with a far detector in Korea

Kaoru Hagiwara¹, Naotoshi Okamura^{2*}, and Ken-ichi Senda^{1†}

¹*KEK Theory Division, and the Graduate University for Advanced Studies (SOKENDAI),
Tsukuba, 305-0801 Japan*

²*Yukawa Institute for Theoretical Physics, Kyoto University,
Kyoto, 606-8502 Japan*

Abstract

We study physics potential of placing a far detector in the east coast of Korea, where the off-axis neutrino beam from J-PARC at Tokai village for the T2K project has significant intensity at a few GeV range. In particular, we examine the capability of determining the mass hierarchy pattern and the CP phase of the lepton-flavor-mixing matrix when a 100 kt water Čerenkov detector is placed at various locations in Korea for the off-axis beam (OAB) of 2.5° and 3° at the Super-Kamiokande site. The best results are found for a combination of 3° OAB at SK ($L = 295\text{km}$) and 0.5° OAB at $L = 1000\text{km}$, where the mass hierarchy pattern can be determined at 3σ level for $\sin^2 2\theta_{\text{RCT}} \gtrsim 0.05$ (0.06) when the hierarchy is normal (inverted), after 5 years of running (5×10^{21} POT). We also find that the leptonic CP phase, δ_{MNS} , can be constrained uniquely, without invoking anti-neutrino beams, as long as the mass hierarchy pattern is determined. Those results are obtained by assuming that the neutrino energy can be reconstructed with a hundred MeV uncertainty for the charged current quasi-elastic events, and the earth matter density along the baseline can be determined with 3% accuracy. We argue that serious studies on possible background to the quasi-elastic events from the neutral current π^0 production processes are mandatory.

*e-mail: okamura@yukawa.kyoto-u.ac.jp

†e-mail: senda@post.kek.jp

1 Introduction

All the results of the neutrino oscillation experiments are consistent with 3 neutrinos except for the LSND [1] experiment. Among the 9 parameters of the three neutrino model, 6 parameters can be measured by neutrino oscillation experiments: 2 mass-squared differences, 3 mixing angles and 1 CP violating phase. As of 2006 spring, we have already known 2 mass-squared differences and 2 mixing angles from the atmospheric neutrino experiments [2], the long-base-line (LBL) neutrino oscillation experiments [3,4], the solar neutrino experiments [5], and the reactor neutrino experiments [6,7]. However, the sign of the larger mass squared-difference ($m_3^2 - m_1^2$), one of the 3 mixing angles (θ_{RCT}), and the CP phase (δ_{MNS}) have not been measured yet. The tasks of the future neutrino oscillation experiments are not only to confirm the 3 neutrino model, but also to measure those unknown parameters of the model.

Here we focus our attention on one of the future neutrino experiments, the Tokai-to-Kamioka experiment (T2K) [8] which will start in 2008. The center of the T2K neutrino beam from J-PARC [9] at Tokai village will go through underground beneath Super-Kamiokande (SK), and reach the sea level east of Korean shore. At the baseline length $L = 295$ km away from Tokai village the upper side of the beam at 2° to 3° off-axis angle is observed at SK, and the lower side of the same beam at 0.5° to 3.0° off-axis angle can be observed in Korea [10]. An additional far detector in Korea can probe the neutrino oscillation at a baseline length (L) of 1000 to 1200 km away from the Tokai village [10–12]. The most welcome feature of this two detector system has been identified [12] as the relative hardness of the neutrino beam energy spectrum at a smaller off-axis angle, which can be observed in the east coast of Korea at $L \sim 1000$ km. Accordingly, it is possible to arrange such that a far detector in Korea probe the oscillation at around the same oscillation phase, $\delta m^2 L / 2E$, at Kamioka. The difference between the resulting two measurements should then come from the difference in the matter effects, which can be a factor of three larger in Korea. In Ref. [12], we showed that the two detector system can resolve the mass hierarchy ambiguity by making use of the strong matter effects on the $\nu_\mu \rightarrow \nu_e$ transition probability [13–16] if a 100 kt level water Čerenkov detector is placed in the east coast of Korea and if the third mixing angle is not too small. It has further been shown in [12] that the leptonic CP phase, δ_{MNS} , can be uniquely constrained once the hierarchy pattern is determined.

In this paper we present details of our findings in Ref. [12]. The paper is organized as follows. In section 2, we review the formalism of the neutrino oscillation including the matter effect, as well as the constraints in the model parameters from the present experimental results. In section 3, we briefly introduce the T2K experiment and discuss merits of the Tokai-to-Kamioka-and-Korea (T2KK) proposal, where an additional large detector is placed in Korea along the T2K neutrino beam baseline. In section 4, we explain details of our analysis method where we select the charged current quasi-elastic events, and a χ^2 function is proposed that takes into account statistical and systematic uncertainties in the experiment, as well as a part of possible background contaminations. In section 5, we show the results of our numerical calculation on the determination of the neutrino mass hierarchy. In section 6, we present our studies on the determination of the CP phase. In section 7, we summarize our findings and give some discussions on the possibility of expanding the T2KK two detector system, and the necessity of further studies on backgrounds which we could not include in the present analysis.

2 Oscillation formulae under the experimental constraints

The neutrino flavor eigenstates, $|\nu_\alpha\rangle$ ($\alpha = e, \mu, \tau$), are related to the mass eigenstates $|\nu_i\rangle$ ($i = 1, 2, 3$) through the lepton-flavor-mixing matrix, or the Maki-Nakagawa-Sakata (MNS) matrix [17]

$$|\nu_\alpha\rangle = U_{\alpha i} |\nu_i\rangle. \quad (1)$$

The probability that an initial flavor eigenstate ν_α with energy E is observed as a flavor eigenstate ν_β after traveling a distance L in the vacuum is expressed as

$$P_{\nu_\alpha \rightarrow \nu_\beta} = |U_{\beta 1} U_{\alpha 1}^* + U_{\beta 2} U_{\alpha 2}^* e^{-i\Delta_{12}} + U_{\beta 3} U_{\alpha 3}^* e^{-i\Delta_{13}}|^2, \quad (2)$$

where the phase Δ_{ij} is

$$\Delta_{ij} = \frac{m_j^2 - m_i^2}{2E} L \simeq 2.534 \frac{(m_j^2 - m_i^2)[\text{eV}^2]}{E[\text{GeV}^2]} L[\text{km}]. \quad (3)$$

Eq. (2) tells us that neutrino oscillation experiments measure the 2 mass-squared differences and the lepton-number conserving contributions of the MNS matrix elements, which can be parametrized by 3 mixing angles and 1 CP violating phase.

The present neutrino oscillation experiments are each sensitive to only one of the 2 mass-squared differences, and the amplitude of each oscillation probability can be expressed in terms of the MNS matrix elements. The atmospheric neutrino oscillation experiments [2] and the long-base line (LBL) neutrino oscillation experiments, K2K [3] and MINOS [4], which measure the ν_μ survival probability, are sensitive to the magnitude of the larger mass-squared difference. The constraints on the mass-squared difference and the amplitude are [2–4]

$$1.5 \times 10^{-3} \text{eV}^2 < |m_3^2 - m_1^2| < 3.4 \times 10^{-3} \text{eV}^2, \quad (4a)$$

$$\sin^2 2\theta_{\text{ATM}} > 0.92, \quad (4b)$$

each at the 90% confidence level. The solar neutrino oscillation experiments [5] and the KamLAND [6] experiment, which measure the ν_e and $\bar{\nu}_e$ survival probability, respectively, are sensitive to the smaller mass-squared difference. The present constraints can be expressed as [6]

$$m_2^2 - m_1^2 = 8.2_{-0.5}^{+0.6} \times 10^{-5} \text{eV}^2, \quad (5a)$$

$$\tan^2 \theta_{\text{SOL}} = 0.40_{-0.07}^{+0.09}. \quad (5b)$$

In the solar neutrino experiments, the sign of $m_2^2 - m_1^2$ is determined by the matter effect in the sun [18,19]. The reactor $\bar{\nu}_e$ experiments at $L \sim 1$ km are sensitive to the oscillation with the larger mass-squared difference. No reduction of the $\bar{\nu}_e$ survival probability has been observed, and the CHOOZ experiment gives the upper limit on the amplitude [7];

$$\sin^2 2\theta_{\text{RCT}} < 0.20 \text{ for } |m_3^2 - m_1^2| = 2.0 \times 10^{-3} \text{eV}^2, \quad (6a)$$

$$\sin^2 2\theta_{\text{RCT}} < 0.16 \text{ for } |m_3^2 - m_1^2| = 2.5 \times 10^{-3} \text{eV}^2, \quad (6b)$$

$$\sin^2 2\theta_{\text{RCT}} < 0.14 \text{ for } |m_3^2 - m_1^2| = 3.0 \times 10^{-3} \text{eV}^2, \quad (6c)$$

at the 90% confidence level.

These observed amplitudes can be identified with the MNS matrix elements as follows [20]. In the atmospheric neutrino experiments and the CHOOZ reactor experiment, $|\Delta_{13}| \sim 1 \gg \Delta_{12}$ is satisfied. Therefore we can set $e^{-i\Delta_{12}} \sim 1$ in eq. (2) and we find the following relations;

$$\begin{aligned} |U_{\mu 3}|^2 &= \sin^2 \theta_{\text{ATM}}, \\ |U_{e 3}|^2 &= \sin^2 \theta_{\text{RCT}}. \end{aligned} \quad (7)$$

As for the solar neutrino experiments and the KamLAND experiment, where the $\Delta_{12} \sim 1$ region is probed, the terms with Δ_{13} oscillate rapidly within the experimental resolution of L/E . After averaging out the Δ_{13} contribution, and by neglecting the term of order $|U_{e 3}|^2$, which is constrained to be smaller than about 0.04 by the CHOOZ experiment [7], eq. (6b), we obtain the relation;

$$4|U_{e 1}U_{e 2}|^2 = \sin^2 2\theta_{\text{SOL}}. \quad (8)$$

These simple identifications, eqs. (7) and (8), are found to give a reasonably good description of the present data in dedicated studies [21] of the experimental constraints in the three neutrino model. In this paper we parametrize the MNS matrix in terms of the three positive numbers, $\sin^2 \theta_{\text{ATM}}$, $\sin^2 \theta_{\text{RCT}}$, and $\sin^2 2\theta_{\text{SOL}}$ with the identification of eqs. (7) and (8), respectively, and the CP phase

$$\delta_{\text{MNS}} = -\arg U_{e 3}. \quad (9)$$

This convention [20] allows us to express the MNS matrix in terms of the three observed amplitudes, directly.

The neutrino oscillation through the earth is complicated by the fact that ν_e and $\bar{\nu}_e$ have the extra W -boson exchange interactions with electrons in the matter [18]. The effect is small at low energies, and an approximation of keeping only the linear terms in the matter effect and the smaller mass-squared difference has been found useful for analyzing the LBL experiments at sub GeV to a few GeV range [22]. We find [12, 23],

$$P_{\nu_\mu \rightarrow \nu_\mu} = 1 - \sin^2 2\theta_{\text{ATM}} (1 + A^\mu) \sin^2 \left(\frac{\Delta_{13}}{2} + B^\mu \right), \quad (10a)$$

$$P_{\nu_\mu \rightarrow \nu_e} = 4 \sin^2 \theta_{\text{ATM}} \sin^2 \theta_{\text{RCT}} (1 + A^e) \sin^2 \left(\frac{\Delta_{13}}{2} + B^e \right). \quad (10b)$$

Here A^α and B^α are, respectively, the correction terms to the amplitude and the oscillation phase: For $\alpha = \mu$, we find

$$A^\mu = -\frac{aL}{\Delta_{13}E} \frac{\cos 2\theta_{\text{ATM}}}{\cos^2 \theta_{\text{ATM}}} \sin^2 \theta_{\text{RCT}}, \quad (11a)$$

$$B^\mu = \frac{aL}{4E} \frac{\cos 2\theta_{\text{ATM}}}{\cos^2 \theta_{\text{ATM}}} \sin^2 \theta_{\text{RCT}} \quad (11b)$$

$$-\frac{\Delta_{12}}{2} \left(\cos^2 \theta_{\text{SOL}} + \tan^2 \theta_{\text{ATM}} \sin^2 \theta_{\text{SOL}} \sin^2 \theta_{\text{RCT}} - \tan \theta_{\text{ATM}} \sin 2\theta_{\text{SOL}} \sin \theta_{\text{RCT}} \cos \delta_{\text{MNS}} \right).$$

For $\alpha = e$, we find

$$A^e = \frac{aL}{\Delta_{13}E} \cos 2\theta_{\text{RCT}} - \frac{\Delta_{12}}{2} \frac{\sin 2\theta_{\text{SOL}}}{\tan \theta_{\text{ATM}} \sin \theta_{\text{RCT}}} \sin \delta_{\text{MNS}}, \quad (12a)$$

$$B^e = -\frac{aL}{4E} \cos 2\theta_{\text{RCT}} + \frac{\Delta_{12}}{2} \left(\frac{\sin 2\theta_{\text{SOL}}}{2 \tan \theta_{\text{ATM}} \sin \theta_{\text{RCT}}} \cos \delta_{\text{MNS}} - \sin^2 \theta_{\text{SOL}} \right). \quad (12b)$$

Here the term a gives the contribution of the extra potential for ν_e

$$a = 2\sqrt{2}G_F E n_e \approx 7.56 \times 10^{-5} \text{ eV}^2 \left(\frac{\rho}{\text{g/cm}^3} \right) \left(\frac{E}{\text{GeV}} \right), \quad (13)$$

where n_e is the number density of the electron and ρ is the matter density.

Substituting typical numbers of the parameters from the atmospheric neutrino experiments and the solar neutrino experiments, summarized in eqs. (4) and (5), and with $\rho = 3.0 \text{ g/cm}^3$, we obtain the following expression for A^μ and B^μ , around the oscillation maximum, $|\Delta_{13}| \sim \pi$:

$$|A^\mu| \lesssim 0.006 \left| 1 - \sin^2 2\theta_{\text{ATM}} \right|^{1/2} \frac{\pi}{|\Delta_{13}|} \frac{L}{295 \text{ km}} \left(\frac{\sin^2 2\theta_{\text{RCT}}}{0.10} \right), \quad (14a)$$

$$B^\mu \sim - \left[0.037 - 0.008 \left(\frac{\sin^2 2\theta_{\text{RCT}}}{0.10} \right)^{1/2} \cos \delta_{\text{MNS}} \right] \frac{|\Delta_{13}|}{\pi}. \quad (14b)$$

The magnitude of A^μ around $|\Delta_{13}| = \pi$ should be smaller than about 2×10^{-3} (6×10^{-3}) at $L = 295$ km (1000 km), according to eqs. (4b) and (6b), and hence the amplitude of the ν_μ survival probability is not affected much by the matter effect. Therefore, we can measure $\sin^2 2\theta_{\text{ATM}}$ rather uniquely from the ν_μ disappearance probability independent of the neutrino mass hierarchy and the other unconstrained parameters. The phase-shift term B^μ affects the measurement of $|m_3^2 - m_1^2|$, whose preferred value grows (decreases) for the normal (inverted) hierarchy, and the magnitude of the shift can be about to 2% (3%) when $\cos \delta_{\text{MNS}} = 1$ (-1) for $\sin^2 2\theta_{\text{RCT}} = 0.1$. In other words, unless we determine the hierarchy, a few percent level of uncertainty should remain as a systematic error of $|m_3^2 - m_1^2|$.

As for the $\nu_\mu \rightarrow \nu_e$ oscillation, eqs. (10b) and (12), we find

$$A^e \sim 0.11 \frac{\pi}{\Delta_{13}} \frac{L}{295 \text{ km}} - \left[0.49 \left(\frac{0.10}{\sin^2 2\theta_{\text{RCT}}} \right)^{1/2} \sin \delta_{\text{MNS}} \right] \frac{|\Delta_{13}|}{\pi}, \quad (15a)$$

$$B^e \sim -0.08 \left(\frac{L}{295 \text{ km}} \right) + \left[0.24 \left(\frac{0.10}{\sin^2 2\theta_{\text{RCT}}} \right)^{1/2} \cos \delta_{\text{MNS}} - 0.02 \right] \frac{|\Delta_{13}|}{\pi}. \quad (15b)$$

From eq. (15a), we find that the amplitude of the oscillation probability is sensitive to the mass hierarchy pattern, because the first term changes sign. Its magnitude increases (decreases) by 11% for the normal (inverted) hierarchy at $L = 295$ km for $\sin \delta_{\text{MNS}} = 0$. The difference between the two hierarchy cases grows with L when L/E is fixed at $|\Delta_{13}| \sim \pi$, reaching $\pm 35\%$ at $L = 1000$ km. The shift is also sensitive to $\sin \delta_{\text{MNS}}$, which can decrease (increase) the amplitude by as much as 50% for $\sin \delta_{\text{MNS}} = 1(-1)$ when $\sin^2 2\theta_{\text{RCT}} = 0.1$, independent of the mass hierarchy. As for the phase-shift term B^e , the oscillation peak energy grows (decreases) with the base-line length L , for the normal (inverted) hierarchy, by about 5% at $L = 295$ km and by about 15% at $L = 1000$ km, for $\cos \delta_{\text{MNS}} = 0$. The $\cos \delta_{\text{MNS}}$ dependence of the shift is also significant, which can be $\pm 15\%$ for $\cos \delta_{\text{MNS}} = \pm 1$ if $\sin^2 2\theta_{\text{RCT}} = 0.1$.

The above observation inspires a two detector system, where both detectors can measure $\nu_\mu \rightarrow \nu_e$ oscillations around the oscillation maximum ($|\Delta_{13}| \sim \pi$) but at significantly different base-line lengths. If the magnitude of the product of $\sin^2 \theta_{\text{ATM}} \sin^2 \theta_{\text{RCT}}$ is large enough that the $\nu_\mu \rightarrow \nu_e$ oscillation is observed at both detectors, then the difference of the observed oscillation probabilities at the two locations determines the mass hierarchy uniquely, and hence also the product $\sin^2 \theta_{\text{ATM}} \sin^2 \theta_{\text{RCT}}$ rather independent of δ_{MNS} . Once the hierarchy is determined, the measurements of the magnitude and the phase of the $\nu_\mu \rightarrow \nu_e$ oscillation measure $\sin \delta_{\text{MNS}}$ and $\cos \delta_{\text{MNS}}$, respectively, and hence the CP violating phase δ_{MNS} can be determined uniquely. In the following section, we will find that the T2KK program indeed satisfies all the above conditions, and our numerical simulation supports the simple picture presented in this section based on the approximate formulae eqs. (10) - (15).

3 Merits of detecting the T2K off-axis beam in Korea

Many neutrino oscillation experiments [24–30] are planned to measure $\sin^2 2\theta_{\text{RCT}}$. Tokai-to-Kamioka (T2K) neutrino-oscillation experiment which will start in 2008 is one of them. In T2K, high intensity ν_μ beam is produced by the proton accelerator which is under construction at J-PARC in Tokai-village. These ν_μ 's are shot to Kamioka, 295 km west from Tokai. Super-Kamiokande (SK) will measure both the $\nu_\mu \rightarrow \nu_\mu$ survival rate and the $\nu_\mu \rightarrow \nu_e$ transition rate. The measurement of the $\nu_\mu \rightarrow \nu_e$ transition probability is the main purpose of the T2K experiment, because it tells us the magnitude of $\sin^2 \theta_{\text{RCT}}$, see eq. (10b), the last unmeasured mixing angle of the 3×3 MNS matrix. In order to observe the signal of $\nu_\mu \rightarrow \nu_e$ clearly, the neutrino beam should satisfy the following conditions.

1. The neutrino energy near the oscillation maximum ($|\Delta_{13}| \sim \pi$) at $L = 295$ km is expected to be around 0.5 GeV to 0.7 GeV according to the present experimental bound, eq. (4). The ν_μ flux should hence be large in this energy region.
2. High energy neutrinos produce π^0 's via neutral current, which become background to the ν_e Charged Current Quasi-Elastic (CCQE) events. Therefore, the flux of ν_μ beam should be small at high energies.

T2K adopts the off-axis beam which satisfies the above requirements [8, 31]. We show the flux of the T2K off-axis ν_μ beam [31] in Fig. 1 (a), for 10^{21} POT/yr at $L = 295$ km for various off-axis angles between 0° and 3° . It is clearly seen that the flux peaks at

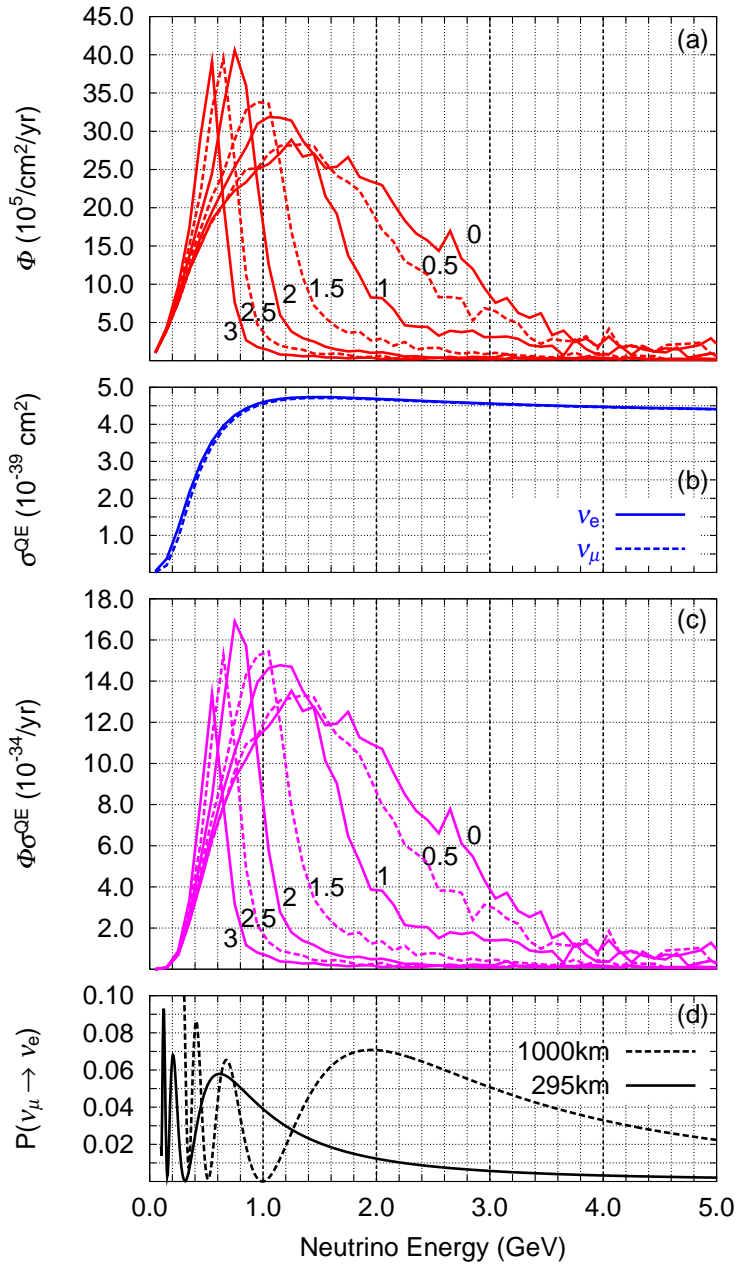


Figure 1: (a). The flux of the T2K ν_μ beam for 10^{21} POT/yr at $L = 295$ km for various off-axis angles between 0° and 3° . (b). The cross section per nucleon of the Charged Current Quasi Elastic (CCQE) events for ν_e and ν_μ off the water target. (c). The flux at 295 km times ν_e CCQE cross section. (d). Probability of $\nu_\mu \rightarrow \nu_e$ transition at 295 km (solid line) and that at 1000 km (dashed line) calculated for $m_3^2 - m_1^2 = 2.5 \times 10^{-3} \text{ eV}^2$, $m_2^2 - m_1^2 = 8.3 \times 10^{-5} \text{ eV}^2$, $\sin^2 2\theta_{\text{ATM}} = 1.0$, $\sin^2 2\theta_{\text{SOL}} = 0.84$, $\sin^2 2\theta_{\text{RCT}} = 0.10$, $\delta_{\text{MNS}} = 0^\circ$, and $\rho = 2.8 \text{ g/cm}^3$ for $L = 295$ km, and $\rho = 3.0 \text{ g/cm}^3$ for $L = 1000$ km.

0.55 to 0.75 GeV at 2° to 3° off-axis angles. In Fig. 1(b) we show the cross section per nucleon of the ν_e and ν_μ CCQE events off the water target [3], and in Fig. 1(c), we show the product of the ν_e CCQE cross section and the ν_μ flux at 295 km for various off-axis angles. Because the neutrino energy reconstruction is essential to determine the oscillation phase, we use only the CCQE events in our analysis. Fig. 1(b) shows that the CCQE cross sections grow quickly above the threshold, become $\sim 3.5 \times 10^{-39} \text{ cm}^2$ at $E_\nu \sim 0.6 \text{ GeV}$, and stay approximately constant at $\sim 4.5 \times 10^{-39} \text{ cm}^2$ at $E_\nu \gtrsim 0.8 \text{ GeV}$ up to $\sim 5 \text{ GeV}$ where the flux diminishes. We also show the typical $\nu_\mu \rightarrow \nu_e$ transition probability at $L = 295 \text{ km}$ and that at $L = 1000 \text{ km}$ in Fig. 1(d), calculated for $m_3^2 - m_1^2 = 2.5 \times 10^{-3} \text{ eV}^2$, $m_2^2 - m_1^2 = 8.3 \times 10^{-5} \text{ eV}^2$, $\sin^2 2\theta_{\text{ATM}} = 1.0$, $\sin^2 2\theta_{\text{SOL}} = 0.84$, $\sin^2 2\theta_{\text{RCT}} = 0.10$, $\delta_{\text{MNS}} = 0^\circ$, and $\rho = 2.8 \text{ g/cm}^3$ for $L = 295 \text{ km}$, and $\rho = 3.0 \text{ g/cm}^3$ for $L = 1000 \text{ km}$. From Fig. 1 (a), (c), and (d), we confirm that the 2.0° to 3.0° off-axis beam (OAB) has a strong flux peak where the oscillation maximum is expected at SK. We also note that the beam at smaller off-axis angles has significant flux in the $1.4 \sim 3 \text{ GeV}$ region where the oscillation maximum of the $\nu_\mu \rightarrow \nu_e$ transition is expected at $L = 1000 \text{ km}$.

During the T2K experimental period, the center of the ν_μ beam from J-PARC goes through Kamioka at 2° to 3° beneath SK, and the lower side of the same beam will appear in Korea at various off-axis angles. We show in Fig. 2 the off-axis angle of the ν_μ beam at the sea level for the 2.5° off-axis beam (a) and 3.0° off-axis beam (b) at SK. The baseline lengths are shown by vertical contours, and the off-axis angles at the sea level are shown by elliptic contours between 0.5° and 3.0° . The SK is slightly off the corresponding contour because it is about 320 m above sea level. We find that, when the 2.5° (3.0°) off-axis beam reaches SK, the 1.0° (0.5°) off-axis beam appears in the east coast of Korea which is 1000 km away from J-PARC. If a huge neutrino detector is constructed in the east coast of Korea, along the T2K beam direction, the two detector system, the Tokai-to-Kamioka-and-Korea (T2KK) experiment, can observe the oscillation maximum of the $\nu_\mu \rightarrow \nu_e$ transition probability at two vastly different base-line lengths.

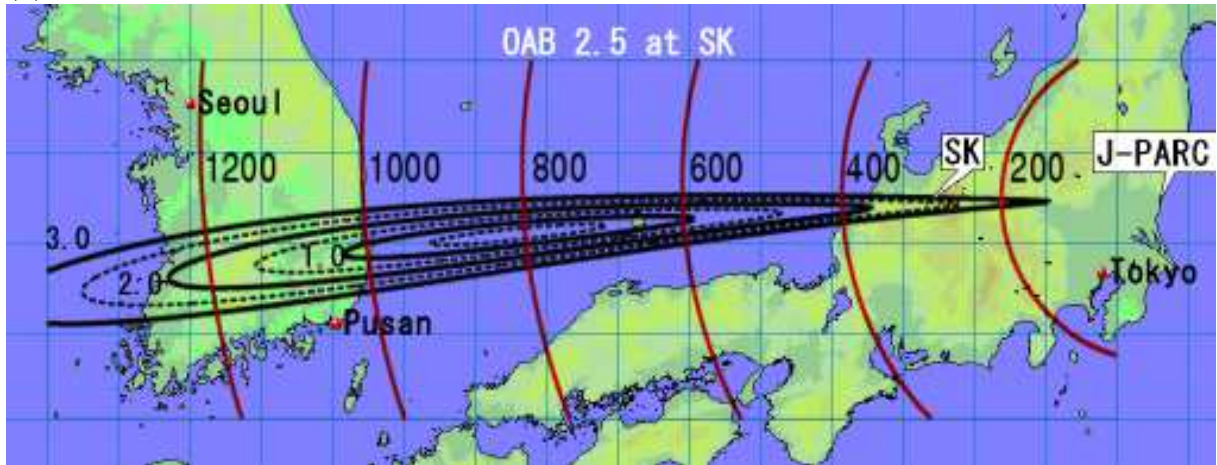
Our most important observation for the T2KK proposal is that the matter effect term in eq. (15a) at Korea is about 3 times as large as that at Kamioka. Because the sign of the matter effect in A^e follows the sign of Δ_{13} , the amplitude of the $\nu_\mu \rightarrow \nu_e$ oscillation for the normal hierarchy at $|\Delta_{13}| \sim \pi$ is larger than that for the inverted hierarchy. Because the matter effect is stronger at Korea, if the probability is found larger (smaller) at Korea than the one at Kamioka, we can conclude that the hierarchy is normal (inverted), irrespective of the other model parameters such as $\sin^2 2\theta_{\text{RCT}}$ and δ_{MNS} [12].

Let us examine this observation semi-quantitatively by using the approximate formulae in eqs. (10) - (15). The difference between the $\nu_\mu \rightarrow \nu_e$ oscillation amplitude (the maximum value of the oscillation probability) at a far detector and that at a near detector is

$$\begin{aligned} \Delta P_{\text{normal}} &= P_{\mu \rightarrow e}(L_{\text{far}}, \Delta_{13} = +\pi) - P_{\mu \rightarrow e}(L_{\text{near}}, \Delta_{13} = +\pi), \\ \Delta P_{\text{inverted}} &= P_{\mu \rightarrow e}(L_{\text{far}}, \Delta_{13} = -\pi) - P_{\mu \rightarrow e}(L_{\text{near}}, \Delta_{13} = -\pi), \end{aligned} \quad (16)$$

respectively, for the normal hierarchy ($\Delta_{13} = +\pi$) and the inverted one ($\Delta_{13} = -\pi$). Then the difference of ΔP between the normal hierarchy and the inverted hierarchy can

(a)



(b)

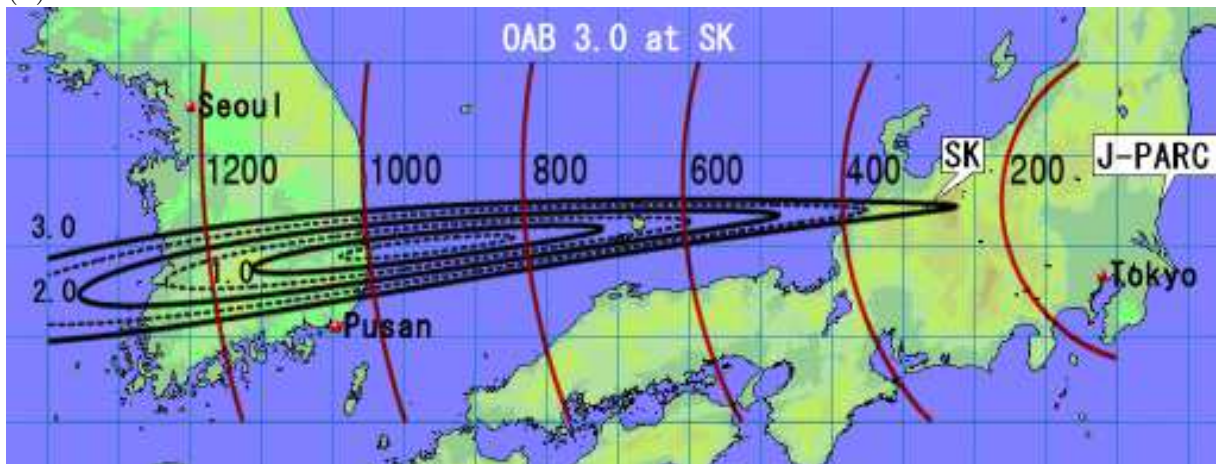


Figure 2: The off-axis angle of the neutrino beam from J-PARC on the sea level, when the beam center is 2.5° (a) and 3.0° (b) off at the SK site. The baseline lengths are shown by vertical contours, and the off-axis angles at the sea level are shown by elliptic contours between 0.5° and 3.0° . The SK is slightly off the corresponding contour because it is about 320 m above sea level.

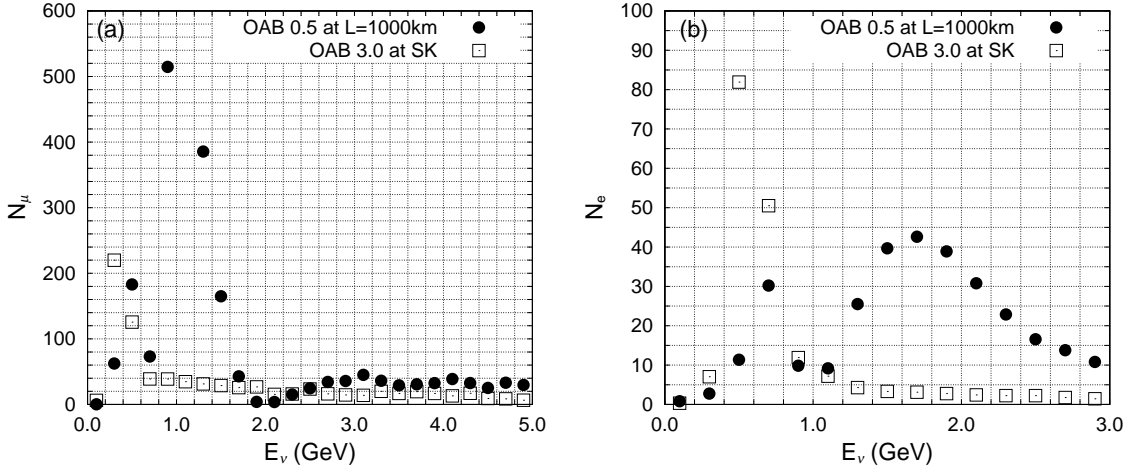


Figure 3: The typical numbers of the μ events (a), and those of the e events (b), for the exposure time of 5 years (5×10^{21} POT), for the 3.0° OAB at SK (open square), and for the 0.5° OAB at $L = 1000$ km with a 100 kt water Čerenkov detector (solid circles). The input parameters are the same as those of Fig. 1 (d).

be expressed as

$$\begin{aligned} \Delta P_{\text{normal}} - \Delta P_{\text{inverted}} &\sim 8 \sin^2 \theta_{\text{ATM}} \sin^2 \theta_{\text{RCT}} \left(\frac{aL_{\text{far}}}{\pi E_{\text{far}}} - \frac{aL_{\text{near}}}{\pi E_{\text{near}}} \right) \\ &\sim 0.01 \left(\frac{\sin^2 2\theta_{\text{RCT}}}{0.10} \right) \left(\frac{L_{\text{far}} - 1}{295 \text{ km}} \right), \end{aligned} \quad (17)$$

where we set $L_{\text{near}} = 295$ km and used the approximation of eqs. (10b), (12b), and (15a). The difference grows linearly with the distance, L_{far} , as long as the oscillation maximum is covered by the flux. When the normal hierarchy is the true hierarchy pattern, the ability of excluding the inverted hierarchy ($\Delta_{13} = -\pi$) is then determined by the error of the ΔP_{normal} , which can be estimated as

$$\begin{aligned} \delta(\Delta P) &= \left[(\delta P_{\mu \rightarrow e}(L = 295 \text{ km}))^2 + (\delta P_{\mu \rightarrow e}(L_{\text{far}}))^2 \right]^{1/2} \\ &= \left[\left(\frac{P_{\mu \rightarrow e}(L = 295 \text{ km})}{\sqrt{N_e^{\text{near}}}} \right)^2 + \left(\frac{P_{\mu \rightarrow e}(L_{\text{far}})}{\sqrt{N_e^{\text{far}}}} \right)^2 \right]^{1/2}. \end{aligned} \quad (18)$$

Here N_e is the number of ν_e appearance events. $N_e^{\text{far}}/N_e^{\text{near}}$ can be expressed as

$$\frac{N_e^{\text{far}}}{N_e^{\text{near}}} = \frac{V_{\text{far}}}{V_{\text{near}}} \frac{\Phi_{\text{far}}(E_\nu \text{ at } \Delta_{13} = \pi, L = L_{\text{far}})}{\Phi_{\text{near}}(E_\nu \text{ at } \Delta_{13} = \pi, L = 295 \text{ km})}, \quad (19)$$

where V denotes the fiducial volume of the detector and $\Phi(E_\nu, L)$ is the neutrino beam flux at L , which is proportional to $(1/L)^2$. The cross section ratio at different energies drops out, because the neutrino cross section of CCQE events is almost constant in the 0.7 - 5 GeV region; see Fig. 1(b). We therefore need to estimate the number of ν_e CCQE events near the oscillation maximum at SK, N_{near} . We show in Fig. 3, typical numbers of expected CCQE events for the μ events (a) and the e events (b), for the 3.0° OAB at SK. The open squares show the expected numbers of events in a 200 MeV wide E_ν bin, after 5 years (5×10^{21} POT), at $\sin^2 2\theta_{\text{RCT}} = 0.1$ and $\delta_{\text{MNS}} = 0^\circ$ for the normal hierarchy, just as in Fig. 1 (d). From the two bins around $E_\nu = 0.6$ GeV in Fig. 3(b), we may estimate $N_{\text{near}} \sim 130$. The significance of excluding the fake hierarchy can then be estimated as

$$\frac{\Delta P_{\text{normal}} - \Delta P_{\text{inverted}}}{\delta(\Delta P)} = 2.3 \left(\frac{\sin^2 2\theta_{\text{RCT}}}{0.10} \right)^{1/2} \left(\frac{L_{\text{far}} - 1}{295 \text{ km}} \right) \left[1 + 0.225 \left(\frac{L_{\text{far}}}{295 \text{ km}} \right)^2 \frac{100 \text{ kt}}{V_{\text{far}}} \right]^{-1/2}. \quad (20)$$

We find that when we put a 100 kt detector at $L = 1000$ km, the significance can exceed the 3σ level in this very rough estimate, which is confirmed in the following numerical studies.

The phase-shift factor B^e of eq. (10b) also contributes to the determination of the neutrino mass hierarchy pattern. Since $\sin^2(x)$ is an even function of x , the magnitude of $|\Delta_{13}/2 + B^e|$ controls the $\nu_\mu \rightarrow \nu_e$ oscillation in eq. (10b). Because the value of $|\Delta_{13}/2 + B^e|$ varies by changing the sign of Δ_{13} , we have the possibility to distinguish the sign of Δ_{13} by measuring the $\nu_\mu \rightarrow \nu_e$ oscillation phase. At Kamioka, however, B^e is governed by the term proportional to $\cos \delta_{\text{MNS}}$; see eq. (15b), and hence the fake hierarchy can reproduce the same $|\Delta_{13}/2 + B^e|$ by changing the sign of $\cos \delta_{\text{MNS}}$. In Korea, the magnitude of the matter effect term in eq. (15a) is almost as large as that of the $\cos \delta_{\text{MNS}}$ terms, and hence the fake hierarchy cannot reproduce the same oscillation phase. When $\cos \delta_{\text{MNS}} \sim 1$, this difference is not effective as a tool to determine the hierarchy, because B^e at Korea is almost zero, see eq. (15). The efficiency of these phase-shift contribution grows with the magnitude of B^e , which grows as $\cos \delta_{\text{MNS}}$ decreases. We find that the effect of the phase difference becomes as important as that of the amplitude difference at $\cos \delta_{\text{MNS}} \sim -1$.

From the above consideration, we observe that it is useful to have a far detector in Korea in the region where the neutrino flux is significant around the $\nu_\mu \rightarrow \nu_e$ oscillation maximum, which is typically between 1.4 GeV to 3 GeV, see Fig. 1(d). Figs. 1 (a) and (c) show that beams at an off-axis angle smaller than 1° have this property. Figs. 2(a) and (b) show that such an off-axis beam will appear in a specific region near the east coast of Korea during the T2K experimental period.

Once the neutrino mass hierarchy is determined, the T2KK experiment also has the ability to measure the leptonic CP phase uniquely without using the anti-neutrino beam. From eqs. (10b) and (15a), there are 2 unmeasured parameters which control the amplitude of $\nu_\mu \rightarrow \nu_e$ oscillation, $\sin^2 \theta_{\text{RCT}}$ and $\sin \delta_{\text{MNS}}$. Due to the significantly different matter effect at $|\Delta_{13}| = \pi$ between Kamioka and Korea, we can constrain both $\sin^2 2\theta_{\text{RCT}}$ and δ_{MNS} uniquely from the two amplitudes. The value of $\cos \delta_{\text{MNS}}$ is measured through the energy dependence of the $\nu_\mu \rightarrow \nu_e$ oscillation probability, through the phase shift B^e ; eq. (15b). Since both $\sin \delta_{\text{MNS}}$ and $\cos \delta_{\text{MNS}}$ can be measured independently,

the CP phase δ_{MNS} can be constrained uniquely.

4 Analysis method

Before we present the results of our numerical calculation, we would like to explain our treatment of the signals and background. In our case study, we consider a 100 kt level detector, in order to compensate for the decrease in the neutrino flux which is about $(300 \text{ km}/1,000 \text{ km})^2 \sim 1/10$ of that at SK. We adopt a Water Čerenkov detector because it allows us to distinguish clearly the e^\pm events from μ^\pm events. We use the CCQE events in our analysis, because it allows us to kinetically reconstruct the neutrino energy event by event. Since the Fermi-motion of the target nucleon dominates the uncertainty of the neutrino energy reconstruction, which is about 80 MeV, we take the width of the energy bin as $\delta E_\nu = 200 \text{ MeV}$ for $E_\nu > 400 \text{ MeV}$, in the following analysis. The signals in the i -th energy bin, $E_\nu^i = 200 \text{ MeV} \times (i+1) < E_\nu < E_\nu^i + \delta E_\nu$, are then calculated as

$$N_\alpha^i(\nu_\mu) = MN_A \int_{E_\nu^i}^{E_\nu^i + \delta E_\nu} \Phi_{\nu_\mu}(E) P_{\nu_\mu \rightarrow \nu_\alpha}(E) \sigma_\alpha^{QE}(E) dE, \quad (21)$$

where $P_{\nu_\mu \rightarrow \nu_\alpha}$ is the neutrino oscillation probability including the matter effect, M is the detector mass, $N_A = 6.017 \times 10^{23}$ is the Avogadro constant, Φ_{ν_μ} is the ν_μ flux from J-PARC [31], and σ_α^{QE} is the CCQE cross section per nucleon in water [3]. The fiducial volume of Super-Kamiokande is 22.5 kt, and we assume that a detector in Korea is 100 kt. The detection efficiencies of both detectors for both ν_μ and ν_e CCQE events are set at 100% for brevity.

We consider the following background events for the signal e - and μ -like events

$$N_\alpha^{i,\text{BG}} = N_\alpha^i(\nu_e) + N_\alpha^i(\bar{\nu}_e) + N_\alpha^i(\bar{\nu}_\mu), \quad (\alpha = e, \mu). \quad (22)$$

The three terms correspond to the contribution from the secondary neutrino flux of the ν_μ primary beam, which are calculated as in eq. (21) where $\Phi_{\nu_\mu}(E)$ is replaced by $\Phi_{\nu_\beta}(E)$ for $\nu_\beta = \nu_e, \bar{\nu}_e, \bar{\nu}_\mu$. All the primary as well as secondary fluxes used in our analysis are obtained from the website [31]. After summing up these background events, the e -like and μ -like events for the i -th bin are obtained as

$$N_\alpha^i = N_\alpha^i(\nu_\mu) + N_\alpha^{i,\text{BG}}, \quad (\alpha = e, \mu). \quad (23)$$

Since our concern is the possibility to distinguish the neutrino mass hierarchy and to constrain the CP phase uniquely, we study how the above ‘data’ can constrain the model parameters by using the χ^2 function

$$\Delta\chi^2 = \chi_{\text{SK}}^2 + \chi_{\text{Kr}}^2 + \chi_{\text{sys}}^2 + \chi_{\text{para}}^2. \quad (24)$$

Here the first two terms, χ_{SK}^2 and χ_{Kr}^2 , measure the parameter dependence of the fit to the SK and the Korean detector data,

$$\chi_{\text{SK,Kr}}^2 = \sum_i \left\{ \left(\frac{(N_e^i)^{\text{fit}} - N_e^i}{\sqrt{N_e^i}} \right)^2 + \left(\frac{(N_\mu^i)^{\text{fit}} - N_\mu^i}{\sqrt{N_\mu^i}} \right)^2 \right\}, \quad (25)$$

where the summation is over all bins from 0.4 GeV to 5.0 GeV for N_μ , 0.4 GeV to 1.2 GeV for N_e at SK, and 0.4 GeV to 2.8 GeV for N_e at Korea. Here $N_{\mu,e}^i$ is the calculated number of events in the i -th bin, and its square root gives the statistical error. We include the contribution of the μ -events in order to constrain the absolute value of Δ_{13} strongly in this analysis, because a small error of Δ_{13} dilutes the phase shift B^e [12, 23]. In our analysis, we calculate $N_{\mu,e}^i$ by assuming the following input parameters:

$$\left. \begin{array}{l} |m_3^2 - m_1^2|^{\text{input}} = 2.5 \times 10^{-3} \text{ eV}^2, \\ (m_2^2 - m_1^2)^{\text{input}} = 8.3 \times 10^{-5} \text{ eV}^2, \\ \sin^2 \theta_{\text{ATM}}^{\text{input}} = 0.5, \\ \sin^2 2\theta_{\text{SOL}}^{\text{input}} = 0.84, \end{array} \right\} \quad (26)$$

with the constant matter density, $\rho^{\text{input}} = 2.8 \text{ g/cm}^3$ along T2K and $\rho^{\text{input}} = 3.0 \text{ g/cm}^3$ for the Tokai-to-Korea baseline, which goes through deeper in the earth than that of T2K. We examine various input values of $\sin^2 2\theta_{\text{RCT}}$, δ_{MNS} , and the sign of $m_3^2 - m_1^2$.

N_i^{fit} is calculated by allowing the model parameters to vary freely and by allowing for systematic errors. In our analysis, we consider 4 types of systematic errors. The first ones are for the overall normalization of each neutrino flux, for which we assign 3% errors,

$$f_{\nu_\beta} = 1 \pm 0.03, \quad (27)$$

for $\nu_\beta = \nu_e, \bar{\nu}_e, \nu_\mu, \bar{\nu}_\mu$, which are taken common for T2K and the Tokai-to-Korea experiment. The second systematic error is for the uncertainty in the matter density, for which we allow 3% overall uncertainty along the baseline, independently for T2K (f_ρ^{SK}) and the Tokai-to-Korea experiment (f_ρ^{Kr}):

$$\rho_i^{\text{fit}} = f_\rho^i \rho_i^{\text{input}} \quad (i = \text{SK, Kr}). \quad (28)$$

The third uncertainty is for the CCQE cross section,

$$\sigma_\alpha^{\text{QE, fit}} = f_\alpha^{\text{QE}} \sigma_\alpha^{\text{QE, input}}. \quad (29)$$

Since ν_e and ν_μ CCQE cross sections are expected to be very similar theoretically, we assign a common overall error of 3% for ν_e and ν_μ ($f_e^{\text{QE}} = f_\mu^{\text{QE}} \equiv f_\ell^{\text{QE}}$), and an independent 3% error for $\bar{\nu}_e$ and $\bar{\nu}_\mu$ CCQE cross sections ($f_{\bar{e}}^{\text{QE}} = f_{\bar{\mu}}^{\text{QE}} \equiv f_{\bar{\ell}}^{\text{QE}}$). The last one is the uncertainty of the fiducial volume, for which we assign 3% error independently for T2K (f_V^{SK}) and the Tokai-to-Korea experiment (f_V^{Kr}). $N_\alpha^{i,\text{fit}}$ is then calculated as

$$\left[N_\alpha^{i,\text{fit}}(\nu_\beta) \right]_{\text{at SK, Kr}} = f_{\nu_\beta} f_\alpha^{\text{QE}} f_V^{\text{SK, Kr}} N_\alpha^i(\nu_\beta), \quad (30)$$

and χ_{sys}^2 has four terms;

$$\chi_{\text{sys}}^2 = \sum_{\alpha=e,\bar{e},\mu,\bar{\mu}} \left(\frac{f_{\nu_\alpha} - 1}{0.03} \right)^2 + \sum_{\alpha=l,\bar{l}} \left(\frac{f_\alpha^{\text{QE}} - 1}{0.03} \right)^2 + \sum_{D=\text{SK, Kr}} \left\{ \left(\frac{f_\rho^i - 1}{0.03} \right)^2 + \left(\frac{f_V^i - 1}{0.03} \right)^2 \right\}. \quad (31)$$

In short, we assign 3% errors for the normalization of each neutrino flux, the ν_l and $\bar{\nu}_l$ CCQE cross sections, the effective matter density along each base line, and for the fiducial volume of SK, and that of the Korean detector.

Finally, χ^2_{para} accounts for the external constraints on the model parameters:

$$\begin{aligned} \chi^2_{\text{para}} = & \left(\frac{|(m_3^2 - m_1^2)^{\text{fit}}| - |(m_3^2 - m_1^2)^{\text{input}}|}{0.5 \times 10^{-3}} \right)^2 + \left(\frac{(m_2^2 - m_1^2)^{\text{fit}} - (m_2^2 - m_1^2)^{\text{input}}}{0.6 \times 10^{-5}} \right)^2 \\ & + \left(\frac{\sin^2 2\theta_{\text{ATM}}^{\text{fit}} - \sin^2 2\theta_{\text{ATM}}^{\text{input}}}{0.04} \right)^2 + \left(\frac{\sin^2 2\theta_{\text{SOL}}^{\text{fit}} - \sin^2 2\theta_{\text{SOL}}^{\text{input}}}{0.07} \right)^2 \\ & + \left(\frac{\sin^2 2\theta_{\text{RCT}}^{\text{fit}} - \sin^2 2\theta_{\text{RCT}}^{\text{input}}}{0.01} \right)^2. \quad (32) \end{aligned}$$

The first four terms correspond to the present experimental constraints summarized in eqs. (4) and (5). In the third term, we interpret the 90% CL lower bound on $\sin^2 2\theta_{\text{ATM}}$ in eq. (4) as the 1.96σ constraint about the best fit value of $\sin^2 2\theta_{\text{ATM}}^{\text{input}} = 1$. In the fourth term the asymmetric error of $\tan^2 \theta_{\text{SOL}}$ in eq. (5) has been made more symmetric for $\sin^2 2\theta_{\text{SOL}}$. In the last term, we assume that the planned future reactor experiments [24, 25] should measure $\sin^2 2\theta_{\text{RCT}}$ with the expected uncertainty of 0.01, during the T2KK experimental period. In total, our $\Delta\chi^2$ function depends on 16 parameters, the 6 model parameters and the 10 normalization factors.

5 Determination of the mass hierarchy pattern

In this section we show the results of our numerical calculation. First, we search for the best combination of the off-axis angle at SK and that at a Korean detector, as well as the base-line length up to Korean detector for determining the sign of $m_3^2 - m_1^2$. For this purpose, we first calculate the expected number of the $\nu_\mu \rightarrow \nu_e$ CCQE events at both detectors by assuming either normal or inverted hierarchy, and then examine if the resulting ‘data’ can be fitted for the opposite hierarchy by adjusting the model parameters.

We show in Fig. 4 the minimum $\Delta\chi^2$ expected at the T2KK two detector experiment after 5 years of running (5×10^{21} POT), as functions of the off-axis angle and the base-line length of the far-detector site from J-PARC at Tokai, when the normal hierarchy ($m_3^2 - m_1^2 > 0$) is assumed in generating the events, and the inverted hierarchy ($m_3^2 - m_1^2 < 0$) is assumed in the fit. The left-hand figure (a) is for the 2.5° OAB at SK, and the right-hand one (b) is for the 3.0° OAB beam at SK. The input parameters are choose as in eq. (26), $\sin^2 2\theta_{\text{RCT}}^{\text{input}} = 0.10$ and $\delta_{\text{MNS}}^{\text{input}} = 0^\circ$. The four symbols, solid circle, open circle, triangle, and square are for $L = 1000\text{km}$, 1050km , 1100km , and 1150km , respectively. There are no data points at 0.5° in Fig. 4(a) for the 2.5° OAB at SK, because the 0.5° off-axis beam does not reach Korea: see Fig. 2(a). It is clearly seen from Fig. 4 that the best combination of off-axis angles are 3° for SK and 0.5° for the Korean detector at $L = 1000$ km. The 0.5° off-axis beam has strong flux up to ~ 2.2 GeV, which overlaps significantly with the broad peak of the $\nu_\mu \rightarrow \nu_e$ oscillation at $L = 1000$ km; see Fig. 1

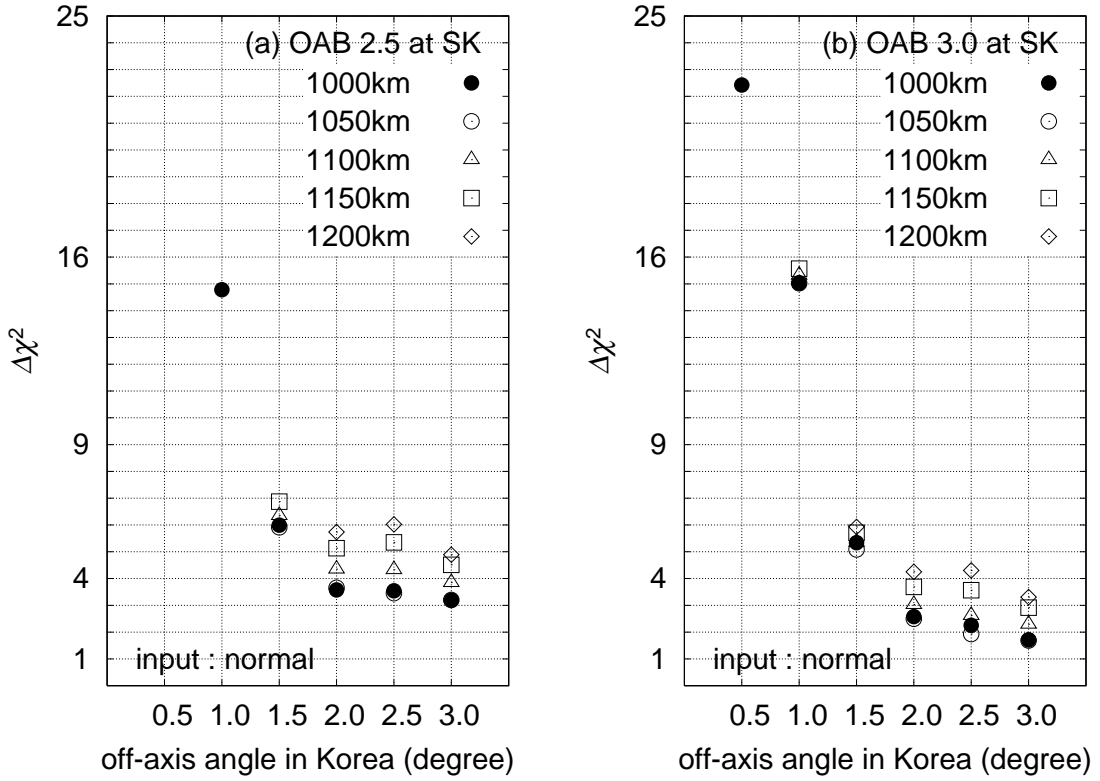


Figure 4: Minimum $\Delta\chi^2$ of the T2KK two detector experiment after 5 years of running (5×10^{21} POT) as functions of the off-axis angle and the base-line length of the far-detector from J-PARC at Tokai, when the normal hierarchy ($m_3^2 - m_1^2 > 0$) is assumed in generating the events, and the inverted hierarchy ($m_3^2 - m_1^2 < 0$) is assumed in the fit. The left-hand figure (a) is for the 2.5° OAB at SK, and the right-hand one (b) is for the 3.0° OAB beam at SK. The input parameters are the same as those of Fig. 1 (d); in particular, $\sin^2 2\theta_{\text{RCT}}^{\text{input}} = 0.10$ and $\delta_{\text{MNS}}^{\text{input}} = 0^\circ$.

(a), (c) and (d). Because the number of the ν_e CCQE events is large enough around the oscillation maximum for $\sin^2 2\theta_{\text{RCT}} \sim 0.1$, both at SK and at the far detector in Korea, we are able to measure the difference in the magnitude of the $\nu_\mu \rightarrow \nu_e$ probability at two vastly different baselines, and can hence distinguish between the normal hierarchy and the inverted hierarchy. We can reject the fake hierarchy at 4.7σ level in our simple simulation with this combination of 3° at SK and 0.5° at $L = 1000$ km.

We find from Fig. 4 that the 1° OAB in Korea still keeps the sensitivity to the neutrino mass hierarchy, where both a combination of 1° at $L = 1000$ km and 2.5° OAB at SK (Fig. 4 (a)) and that of 1° at $L = 1000$ km ~ 1150 km and the 3° OAB at SK (Fig. 4 (b)) distinguish the neutrino mass hierarchy nearly at 4σ level in our simulation. This is because the CCQE cross section times the flux of 1° OAB extends to ~ 1.7 GeV, see Fig. 1 (a) and (c), which barely overlaps with the broad peak region of the $\nu_\mu \rightarrow \nu_e$ oscillation probability shown in Fig. 1(d). From Fig. 2 (a) and (b), we find that the 1° OAB is observable only in the east coast of Korea ($L \sim 1000$ km) for the 2.5° OAB at SK, whereas for the 3° OAB at SK, it can be observed at various base-line lengths up to ~ 1150 km. The small values of $\Delta\chi^2$ for larger off-axis angles in

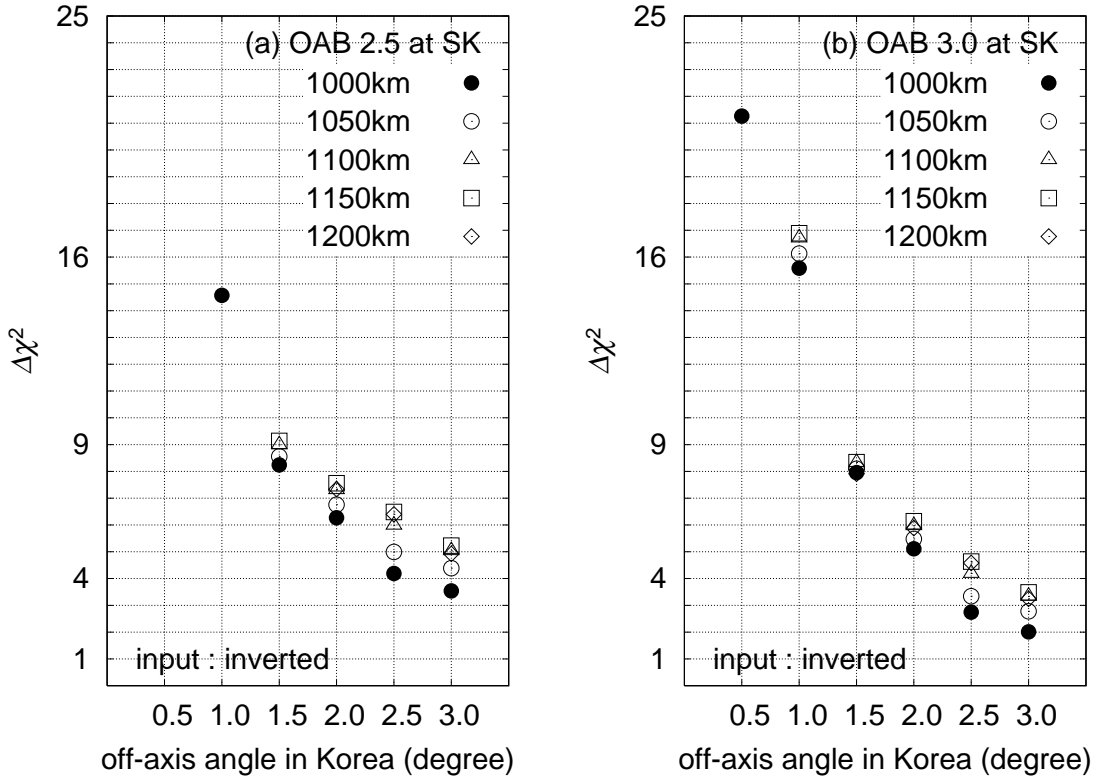


Figure 5: The same as Fig. 4, but when the input data is calculated for the inverted hierarchy ($m_3^2 - m_1^2 < 0$) and the fit is performed by assuming the normal hierarchy ($m_3^2 - m_1^2 > 0$). All the other parameters are the same as those in Fig. 4.

Fig. 4 tell us that it is essential to choose the location of the detector in Korea where the off-axis angle is smaller than 1° .

Fig. 5 is the same as Fig. 4, but when the input data is calculated for the inverted hierarchy and the fit is performed by assuming the normal hierarchy. It is remarkable that almost the same level of the capability to distinguish the neutrino mass hierarchy can be achieved for the OAB $\lesssim 1^\circ$ at $L \sim 1000$ km even when the hierarchy is inverted ($m_3^2 - m_1^2 < 0$). Slight decreases of the minimum $\Delta\chi^2$ value of the best combinations, 23.5 in Fig. 4(b) to 21.3 in Fig. 5(b), and 14.8 in Fig. 4(a) to 14.6 in Fig. 5(a), can be attributed to the smaller expected number of the ν_e appearance events because of the matter effect which suppresses the probability in the inverted hierarchy. We may conclude that a far detector that observes the T2K neutrino beam at $L \sim 1000$ km and the off-axis angle $\lesssim 1^\circ$ has the potential to determine the neutrino mass hierarchy whether it is normal or inverted.

Because we find from Fig. 4 and Fig. 5 that a combination of 0.5° OAB at $L \sim 1000$ km and the 3° OAB at SK has a significantly better capability of determining the neutrino mass hierarchy, we study in the following physics potential of this preferred T2KK set up in more detail. In particular, we investigate the whole un-explored parameter space of the three neutrino model.

First in Fig. 6, we summarize our findings on the capability of the T2KK experiment to determine the neutrino mass hierarchy in the whole space of $\sin^2 2\theta_{\text{RCT}}$ and

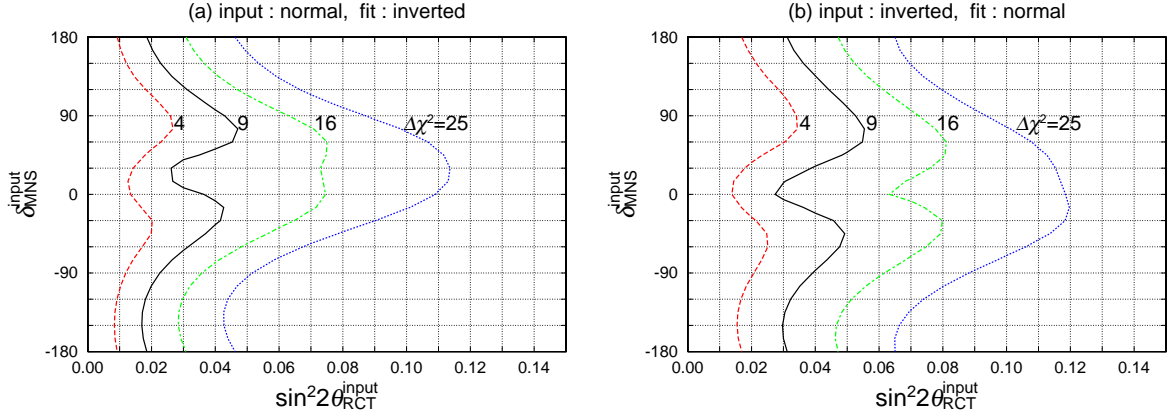


Figure 6: Capability of the T2KK two-detector experiment to determine the neutrino mass hierarchy, (a) when the mass hierarchy is normal ($m_3^2 - m_1^2 > 0$), and (b) when it is inverted ($m_3^2 - m_1^2 < 0$). The numerical results are obtained for a combination of 3.0° OAB at SK and 0.5° off-axis at $L = 1000\text{km}$ with a 100 kt water Čerenkov detector, after 5 years of running (5×10^{21} POT). In each figure the input data are calculated for the model parameters at various $\sin^2 2\theta_{\text{RCT}}^{\text{input}}$ and $\delta_{\text{MNS}}^{\text{input}}$, and the fit has been performed by surveying the whole parameter space with the opposite mass hierarchy. The resulting values of minimum $\Delta\chi^2$ are shown as contours for 2, 3, 4, and 5σ . The wrong hierarchy can be excluded with the corresponding confidence level if the true $\sin^2 2\theta_{\text{RCT}}$ and δ_{MNS} values lie in the right-hand side of each contour. The model parameters are set at $(m_3^2 - m_1^2)^{\text{input}} = 2.5 \times 10^{-3}\text{eV}^2$ (a), $-2.5 \times 10^{-3}\text{eV}^2$ (b), $(m_2^2 - m_1^2)^{\text{input}} = 8.3 \times 10^{-5}\text{eV}^2$, $\sin^2 2\theta_{\text{ATM}}^{\text{input}} = 1.0$, $\sin^2 2\theta_{\text{SOL}}^{\text{input}} = 0.84$, $\rho^{\text{input}} = 2.8\text{g/cm}^3$ for SK, and $\rho^{\text{input}} = 3.0\text{g/cm}^3$ for $L = 1000\text{km}$.

δ_{MNS} . Fig. 6(a) shows our result when the mass hierarchy is normal ($m_3^2 - m_1^2 > 0$), and (b) when it is inverted ($m_3^2 - m_1^2 < 0$). In each figure the input data are calculated for the model parameters at various $\sin^2 2\theta_{\text{RCT}}^{\text{input}}$ and $\delta_{\text{MNS}}^{\text{input}}$ points, and the fit has been performed by surveying the whole parameter space, but under the opposite mass hierarchy. The resulting values of the minimum $\Delta\chi^2$ are shown as contours for 2, 3, 4, and 5σ . The wrong mass hierarchy can be excluded with the corresponding confidence level if the true $\sin^2 2\theta_{\text{RCT}}$ value lies in the right-hand side of each contour along the true value of δ_{MNS} ($\delta_{\text{MNS}}^{\text{input}}$). In particular, the minimum $\Delta\chi^2$ values of 22 for the point $(\sin^2 2\theta_{\text{RCT}}^{\text{input}}, \delta_{\text{MNS}}^{\text{input}}) = (0.10, 0^\circ)$ in Fig. 6(a) corresponds to the highest point in Fig. 4(b), and the corresponding value of 21 in Fig. 6(b) is the highest point in Fig. 5(b). We find that the wrong hierarchy can be excluded at the 3σ level if $\sin^2 2\theta_{\text{RCT}}^{\text{input}} > 0.05$ (0.06) if the hierarchy is normal (inverted).

It is remarkable that the $\delta_{\text{MNS}} = 0^\circ$ case chosen to plot Fig. 4 and Fig. 5 turns out to be the case when it is most difficult to determine the neutrino mass hierarchy. If $\delta_{\text{MNS}} = 180^\circ$, the wrong hierarchy can be excluded at the 3σ level for $\sin^2 2\theta_{\text{RCT}}^{\text{input}} \gtrsim 0.02$ for the normal hierarchy (Fig. 6(a)) or $\sin^2 2\theta_{\text{RCT}}^{\text{input}} \gtrsim 0.03$ for the inverted hierarchy (Fig. 5(b)). The origin of the δ_{MNS} dependence is the difference of the oscillation phase at the far detector in Korea. From eqs. (10b) and (15b), the difference of the oscillation phase near

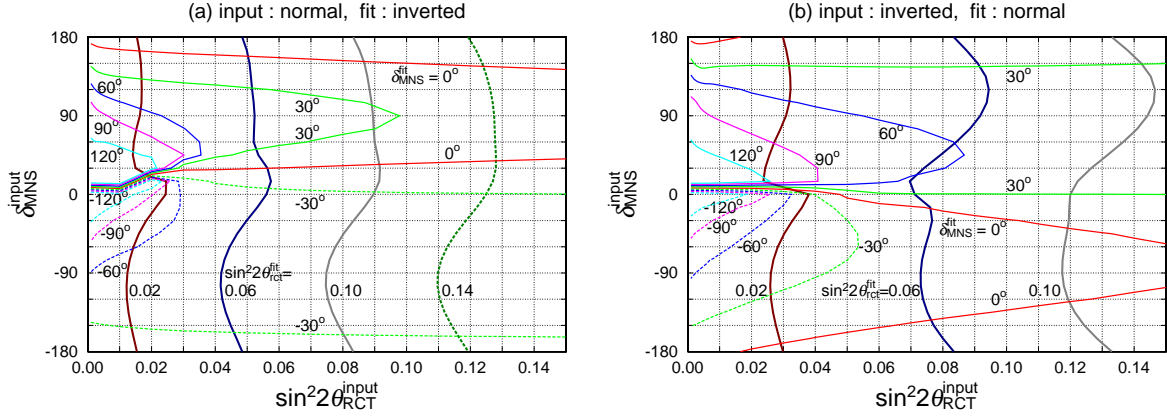


Figure 7: The values of the fit parameters, $\sin^2 2\theta_{\text{RCT}}^{\text{fit}}$ and $\delta_{\text{MNS}}^{\text{fit}}$, at the minimum $\Delta\chi^2$ point of the analysis of Fig. 6 are shown. The results for the normal hierarchy (a) and those for the inverted hierarchy (b) are shown correspondingly to the fit of Fig. 6 (a) and Fig. 6 (b), respectively. The thick vertical lines are the $\sin^2 2\theta_{\text{RCT}}^{\text{fit}}$ contours at 0.02, 0.06, 0.10, and 0.14. The thinner contours give the $\delta_{\text{MNS}}^{\text{fit}}$ values.

the oscillation maximum, $|\Delta_{13}| = \pi$, between the input and the fit is expressed as,

$$\begin{aligned}
& \left| \frac{\Delta_{13}}{2} + B_{\text{input}}^e \right| - \left| -\frac{\Delta_{13}}{2} + B_{\text{fit}}^e \right| \\
& \sim \pm 0.24 \left\{ \cos \delta_{\text{MNS}}^{\text{input}} \left(\frac{0.10}{\sin^2 2\theta_{\text{RCT}}^{\text{input}}} \right)^{1/2} + \cos \delta_{\text{MNS}}^{\text{fit}} \left(\frac{0.10}{\sin^2 2\theta_{\text{RCT}}^{\text{fit}}} \right)^{1/2} \right\} \left(\frac{|\Delta_{13}|}{\pi} \right) \\
& \mp 0.54 \left(\frac{L}{1000 \text{ km}} \right). \tag{33}
\end{aligned}$$

The upper sign is for the normal hierarchy, and the lower sign is for the inverted hierarchy. The phase-shift difference depends on both $\cos \delta_{\text{MNS}}^{\text{input}}$ and $\cos \delta_{\text{MNS}}^{\text{fit}}$. As explained in section 3, below eq. (20), when $\cos \delta_{\text{MNS}}^{\text{input}} \sim 1$ ($\delta_{\text{MNS}}^{\text{input}} \sim 0^\circ$) the phase shift tends to vanish at $L = 1000$ km. Therefore the fitted value of $\cos \delta_{\text{MNS}}^{\text{fit}}$ ($\cos \delta_{\text{MNS}}^{\text{input}}$) also tends to be large and has the opposite sign for the fake hierarchy. If $\cos \delta_{\text{MNS}}^{\text{input}} \sim -1$, it is not possible to compensate for the phase-shift difference of eq. (33) even by choosing $\cos \delta_{\text{MNS}}^{\text{fit}} = 1$, and the significantly higher minimum $\Delta\chi^2$ value results in Fig. 6(a) and (b). In general, $\cos \delta_{\text{MNS}}^{\text{fit}} > 0$ is favored even when $\cos \delta_{\text{MNS}}^{\text{input}} < 0$ in order to minimize the phase-shift difference of eq. (33). This is clearly seen in Fig. 7, where we show the values of the best fit parameters, $\sin^2 2\theta_{\text{RCT}}^{\text{fit}}$ and $\delta_{\text{MNS}}^{\text{fit}}$, at the minimum $\Delta\chi^2$ point of the analysis of Fig. 6. The results for the normal hierarchy (a) and those for the inverted hierarchy (b), are shown correspondingly to the fit of Fig. 6(a) and Fig. 6(b), respectively. The thick vertical lines represent the $\sin^2 2\theta_{\text{RCT}}^{\text{fit}}$ contours at 0.02, 0.06, 0.10 and 0.14. The thinner contours give the $\delta_{\text{MNS}}^{\text{fit}}$ values. We find that the value of $\delta_{\text{MNS}}^{\text{fit}}$ around 0° is almost always favored as expected.

Here let us try to explain more detailed features of Fig. 6 and Fig. 7 by separating

the parameter space of $\sin^2 2\theta_{\text{RCT}}^{\text{input}}$ and $\delta_{\text{MNS}}^{\text{input}}$ into 4 regions.

1. small $\sin^2 2\theta_{\text{RCT}}^{\text{input}}$ region ($\sin^2 2\theta_{\text{RCT}}^{\text{input}} < 0.04$) at any $\delta_{\text{MNS}}^{\text{input}}$: In this region the phase difference eq. (33) is mainly controlled by the $\cos \delta_{\text{MNS}}$ terms, because of the $1/\sqrt{\sin^2 2\theta_{\text{RCT}}}$ enhancement over the matter effect term. It is hence relatively easy to make the difference small by adjusting $\cos \delta_{\text{MNS}}^{\text{fit}} + \cos \delta_{\text{MNS}}^{\text{input}} \sim 0$. The hierarchy is determined essentially by the difference of the $\nu_\mu \rightarrow \nu_e$ oscillation amplitude only.
2. $\sin^2 2\theta_{\text{RCT}}^{\text{input}} \gtrsim 0.04$ at $\delta_{\text{MNS}}^{\text{input}} \sim 180^\circ$: Although the effect of $\cos \delta_{\text{MNS}}^{\text{input}} \sim -1$ is canceled by choosing $\cos \delta_{\text{MNS}}^{\text{fit}} \sim +1$, the difference from the matter effect term in eq. (33) cannot be canceled. Therefore in this region the hierarchy is determined by the differences of both the amplitude and the oscillation phase.
3. $\sin^2 2\theta_{\text{RCT}}^{\text{input}} \gtrsim 0.04$ at $\delta_{\text{MNS}}^{\text{input}} \sim \pm 90^\circ$: In eq. (33), the difference is controlled by the matter effect term and the $\cos \delta_{\text{MNS}}^{\text{fit}}$ term because $\cos \delta_{\text{MNS}}^{\text{input}} \sim 0$. In this region, we can make the phase-shift difference small by choosing $\cos \delta_{\text{MNS}}^{\text{fit}} > 0$.
4. $\sin^2 2\theta_{\text{RCT}}^{\text{input}} \sim 0.04$ to 0.08 at $\delta_{\text{MNS}}^{\text{input}} \sim 0^\circ$: In this region the phase-shift difference eq. (33) at $|\Delta_{13}| \sim \pi$ can be made small at $\cos \delta_{\text{MNS}}^{\text{fit}} \sim 1$, but the difference at $|\Delta_{13}| \sim 2\pi$ becomes large. Because the flux of 0.5° off-axis beam is strong at lower energies where $\pi < |\Delta_{13}| < 2\pi$, the growth of the phase-shift difference eq. (33) at larger $|\Delta_{13}|$ cannot be compensated. This explains why the minimum $\Delta\chi^2$ value in this region is larger than the one for the case 3.

The systematics of the oscillation phase is rather complicated, but its effect turns out to be significant in determining the neutrino mass hierarchy.

Before closing the section, let us briefly study the value of $\sin^2 2\theta_{\text{RCT}}^{\text{fit}}$ in Fig. 7. In Fig. 7(a), $\sin^2 2\theta_{\text{RCT}}^{\text{fit}}$ is larger than $\sin^2 2\theta_{\text{RCT}}^{\text{input}}$, whereas in Fig. 7(b), $\sin^2 2\theta_{\text{RCT}}^{\text{fit}}$ is smaller than $\sin^2 2\theta_{\text{RCT}}^{\text{input}}$. This is because the same oscillation amplitude can be obtained by choosing $\sin^2 2\theta_{\text{RCT}}^{\text{fit}} > \sin^2 2\theta_{\text{RCT}}^{\text{input}}$ when the hierarchy is normal but it is assumed to be inverted in the fit, and *vice versa* for the opposite case. The fitted value of $\sin^2 2\theta_{\text{RCT}}^{\text{input}}$ cannot deviate too much from the input value of $\sin^2 2\theta_{\text{RCT}}^{\text{input}}$, however, because of the constraint from the proposed reactor experiments, according to the last term in eq. (32), and also because of the SK measurement of the $\nu_\mu \rightarrow \nu_e$ probability, which is much less sensitive to the mass hierarchy difference.

6 Measurement of the CP phase

In this section we investigate the measurement of $\sin^2 2\theta_{\text{RCT}}$ and δ_{MNS} for our preferred combination of the 3° OAB at SK and 0.5° OAB at $L = 1000$ km. This combination of the T2KK experiment allows us to measure the $\nu_\mu \rightarrow \nu_e$ oscillation around the oscillation maximum at two base-line lengths, which can be parametrized as in eq. (10b), in terms of the amplitude shift eq. (15a) and the phase shift eq. (15b). Once the neutrino mass hierarchy is determined as explained in the previous section, the terms proportional to $|\Delta_{13}|/\pi$ in the amplitude shift eq. (15a) measure $\sin \delta_{\text{MNS}}$, and those in the phase shift eq. (15b) measure $\cos \delta_{\text{MNS}}$. In the T2KK two detector system, both $\sin^2 2\theta_{\text{RCT}}$ and

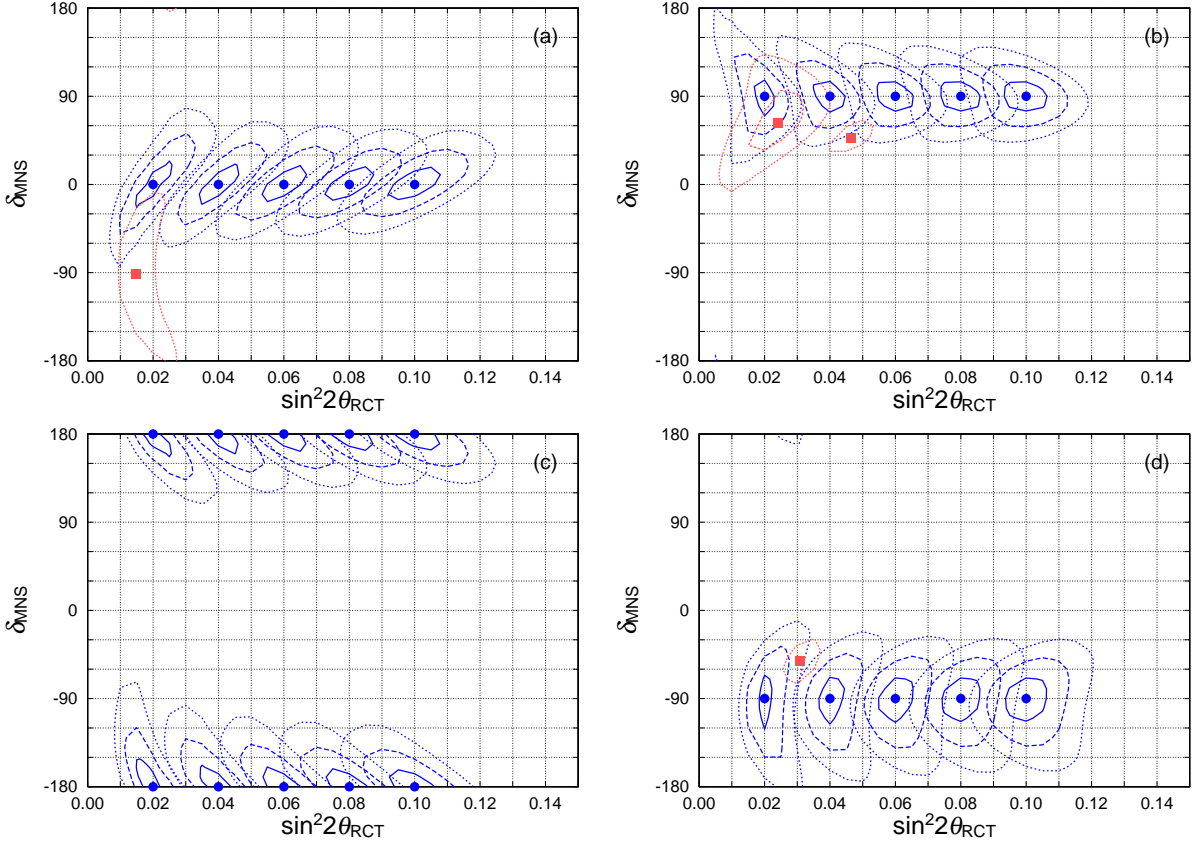


Figure 8: Capability of the T2KK two detector experiment for measuring $\sin^2 2\theta_{\text{RCT}}$ and δ_{MNS} . Allowed regions in the plane of $\sin^2 2\theta_{\text{RCT}}$ and δ_{MNS} are shown for a combination of 3.0° OAB at SK and 0.5° at $L = 1000\text{km}$ with a 100 kt water Čerenkov detector after 5 years of running (5×10^{21} POT). The input values of $\sin^2 2\theta_{\text{RCT}}$ are 0.02, 0.04, 0.06, 0.08 and 0.10 for $\delta_{\text{MNS}} = 0^\circ$ (a), 90° (b), 180° (c), and -90° (d). The normal hierarchy is assumed at $m_3^2 - m_1^2 = 2.5 \times 10^{-3}\text{eV}^2$, and the other parameters are the same as those in Fig. 6. The input points are shown as solid blobs, where $\Delta\chi^2 = 0$ by definition. The 1-, 2-, and 3- σ contours are then shown by solid, dashed, and dotted lines, respectively. For the input values of $(\sin^2 2\theta_{\text{RCT}}^{\text{input}}, \delta_{\text{MNS}}^{\text{input}}) = (0.02, 0^\circ)$ (a), $(0.02, 90^\circ)$ and $(0.04, 90^\circ)$ (b) and $(0.02, -90^\circ)$ (d), there appear additional allowed regions when the mass hierarchy is chosen with the wrong sign in the fit, where the local minimal $\Delta\chi^2$ point is depicted by a solid square.

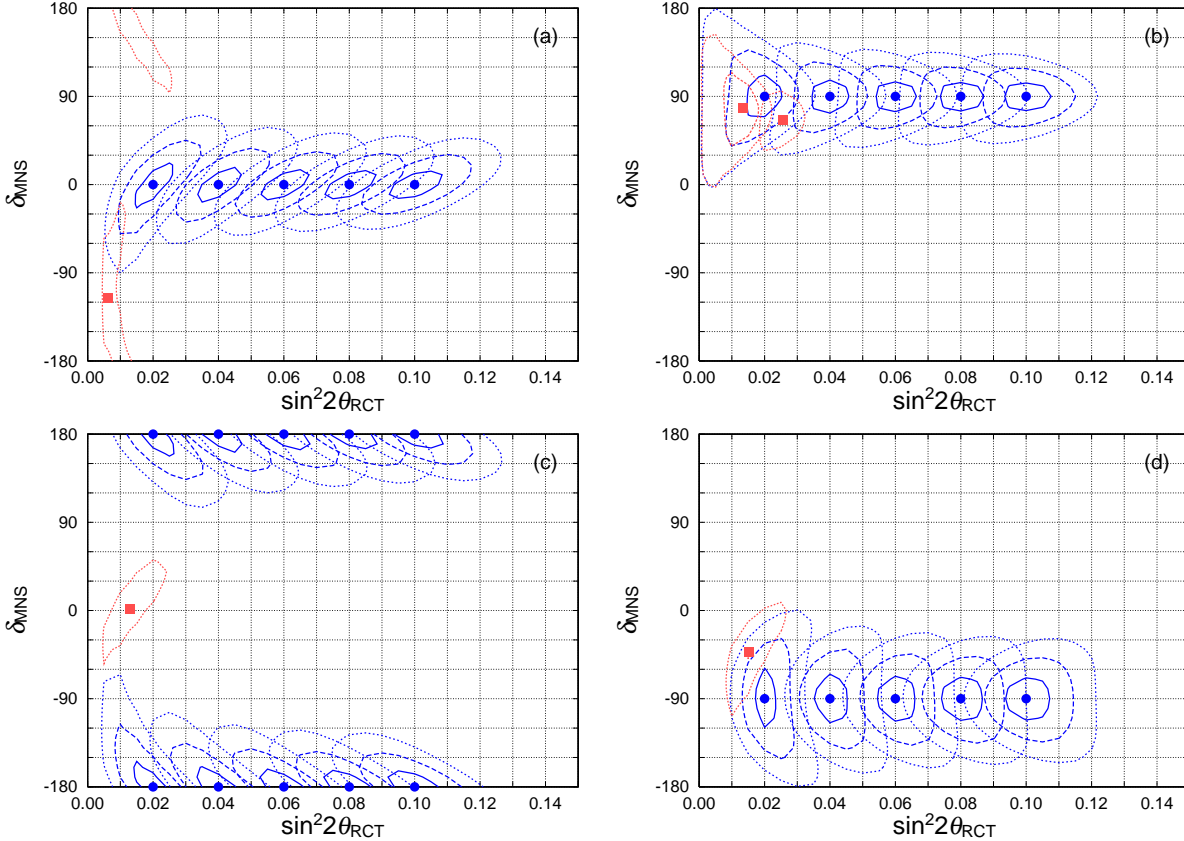


Figure 9: The same as Fig. 8, but when the events are calculated for the inverted hierarchy, *i.e.*, $m_3^2 - m_1^2 = -2.5 \times 10^{-3} \text{ eV}^2$. Just like in Fig. 8, additional allowed regions, when the wrong sign of the $m_3^2 - m_1^2$ is chosen in the fit, appear for all the $\delta_{\text{MNS}}^{\text{input}}$ cases at $\sin^2 2\theta_{\text{RCT}}^{\text{input}} = 0.02$, and for $\delta_{\text{MNS}}^{\text{input}} = 90^\circ$ (b) at $\sin^2 2\theta_{\text{RCT}}^{\text{input}} = 0.04$.

$\sin \delta_{\text{MNS}}$ can be determined uniquely because the amplitude shift eq. (15a) has significantly different matter effect contributions between SK and the far detector. The phase shift measurement of the term eq. (15b) constrains $\cos \delta_{\text{MNS}}$ independent of $\sin \delta_{\text{MNS}}$.

We show in Fig. 8 and Fig. 9 regions allowed by this experiment in the plane of $\sin^2 2\theta_{\text{RCT}}$ and δ_{MNS} . The mean values of the input data are calculated for the parameters of eq. (26). In each figure, input points $(\sin^2 2\theta_{\text{RCT}}^{\text{input}}, \delta_{\text{MNS}}^{\text{input}})$ are shown by solid-circles for $\sin^2 2\theta_{\text{RCT}}^{\text{input}}$ between 0.02 and 0.1, with an interval of 0.02, and for four values of $\delta_{\text{MNS}}^{\text{input}}$; 0° (a), 90° (b), 180° (c), and -90° (d). The regions where the minimum $\Delta\chi^2$ value is less than 1, 4, 9 are depicted by solid, dashed, and dotted boundaries, respectively. Fig. 8 is for the normal hierarchy, and Fig. 9 is for the inverted hierarchy. From these figures, we find that δ_{MNS} can be constrained to $\pm 30^\circ$ at 1- σ level, when $\sin^2 2\theta_{\text{RCT}}^{\text{input}} \gtrsim 0.02$ as long as the neutrino mass hierarchy is determined.

As shown in Fig. 6(a) and (b), the mass hierarchy cannot be determined at 3- σ level ($\Delta\chi^2 > 9$) when $\sin^2 2\theta_{\text{RCT}}^{\text{input}}$ is too small. In case of the input parameters of Fig. 8 for the normal hierarchy, this is the case for $\sin^2 2\theta_{\text{RCT}}^{\text{input}} = 0.02$ at $\delta_{\text{MNS}}^{\text{input}} = 0^\circ$ (a), $\sin^2 2\theta_{\text{RCT}}^{\text{input}} = 0.02$ and 0.04 at $\delta_{\text{MNS}}^{\text{input}} = 90^\circ$ (b), and $\sin^2 2\theta_{\text{RCT}}^{\text{input}} = 0.02$ at $\delta_{\text{MNS}}^{\text{input}} = -90^\circ$ (d). For those input points, there appear an additional allowed region whose center (local minimum of $\Delta\chi^2$) is shown by a solid square. No extra allowed region appears for $\delta_{\text{MNS}} = 180^\circ$ in Fig. 8(c), in accordance with the result of Fig. 6(a). In case of Fig. 9 for

the inverted hierarchy, the local minimum appears for $\sin^2 2\theta_{\text{RCT}}^{\text{input}} = 0.02$ at $\delta_{\text{MNS}}^{\text{input}} = 0^\circ$ (a), $\sin^2 2\theta_{\text{RCT}}^{\text{input}} = 0.02$ and 0.04 at $\delta_{\text{MNS}}^{\text{input}} = 90^\circ$ (b), $\sin^2 2\theta_{\text{RCT}}^{\text{input}} = 0.02$ at $\delta_{\text{MNS}}^{\text{input}} = 180^\circ$ (c), and $\sin^2 2\theta_{\text{RCT}}^{\text{input}} = 0.02$ at $\delta_{\text{MNS}}^{\text{input}} = -90^\circ$ (d).

It is remarkable that the error of δ_{MNS} is almost independent of $\sin^2 2\theta_{\text{RCT}}^{\text{input}}$ value between 0.02 and 0.1, for all the four input values of $\delta_{\text{MNS}}^{\text{input}}$, 0° , $\pm 90^\circ$, and 180° . This is remarkable because the event number N_e is proportional to $\sin^2 2\theta_{\text{RCT}}$ according to eq. (10b), and hence the statistical error of the measurement of the amplitude and the phase should be proportional to $1/\sqrt{N_e}$, or $1/\sqrt{\sin^2 \theta_{\text{RCT}}}$. This increase in the error for small $\sin^2 2\theta_{\text{RCT}}^{\text{input}}$ values is canceled by the increased sensitivities of both the amplitude and the phase shift to $\sin \delta_{\text{MNS}}$ and $\cos \delta_{\text{MNS}}$, respectively, which are both proportional to $1/\sqrt{\sin^2 \theta_{\text{RCT}}}$. The two effects cancel rather accurately, and we find that the error of δ_{MNS} is almost independent of the input values of $\sin^2 2\theta_{\text{RCT}}$ and δ_{MNS} .

7 Conclusion and discussions

In this paper we study physics potential of the T2KK proposal [10–12], where a far detector along the T2K neutrino beam line is placed in Korea. We find that the off-axis neutrino beam from J-PARC at Tokai village for the T2K project has significant intensity at a few GeV range when the far detector is placed in the east coast of Korea where the beam at less than 1° off-axis can be observed at a base-line length of $L \sim 1000$ km. The resulting two detector system can observe the $\nu_\mu \rightarrow \nu_e$ oscillation probability near the oscillation maximum at two different energies, if $\sin^2 2\theta_{\text{RCT}}$ is not too small.

We examine, in particular, the capability of determining the mass hierarchy pattern and the CP phase of the lepton-flavor-mixing matrix when a 100 kt water Čerenkov detector is placed at various locations in Korea for the off-axis beam (OAB) of 2.5° and 3° at the Super-Kamiokande site. The best results are found for a combination of 3° OAB at SK ($L = 295$ km) and 0.5° OAB at $L = 1000$ km, where the mass hierarchy pattern can be determined at 3σ level for $\sin^2 2\theta_{\text{RCT}} \gtrsim 0.05$ (0.06) when the hierarchy is normal (inverted), after 5 years of running (5×10^{21} POT). The sensitivity of the T2KK experiment on the neutrino mass hierarchy depends not only on $\sin^2 2\theta_{\text{RCT}}$ but also on δ_{MNS} . We explore the sensitivity in the whole space of $\sin^2 2\theta_{\text{RCT}}$ and δ_{MNS} , and the results are shown in Fig. 6(a) for the normal hierarchy and in Fig. 6(b) for the inverted hierarchy. Significantly higher sensitivity is found for $\delta_{\text{MNS}} \sim 180^\circ$ for both hierarchy cases.

We also find that the leptonic CP phase, δ_{MNS} , can be constrained uniquely, without invoking anti-neutrino beams, as long as the mass hierarchy pattern is determined: see Fig. 8 for the normal hierarchy, and Fig. 9 for the inverted hierarchy.

Those results are obtained by assuming that the neutrino energy can be reconstructed with a hundred MeV uncertainty for the charged current quasi-elastic events, and the earth matter density along the baseline can be determined with 3% accuracy. All our numerical results have been understood semi-quantitatively, by using the approximative expression for the $\nu_\mu \rightarrow \nu_\mu$ and $\nu_\mu \rightarrow \nu_e$ oscillation probabilities, eqs. (10), (11), and (12), where only the linear terms in the matter effect and those in $\sin^2 2\theta_{\text{RCT}}$ are kept in

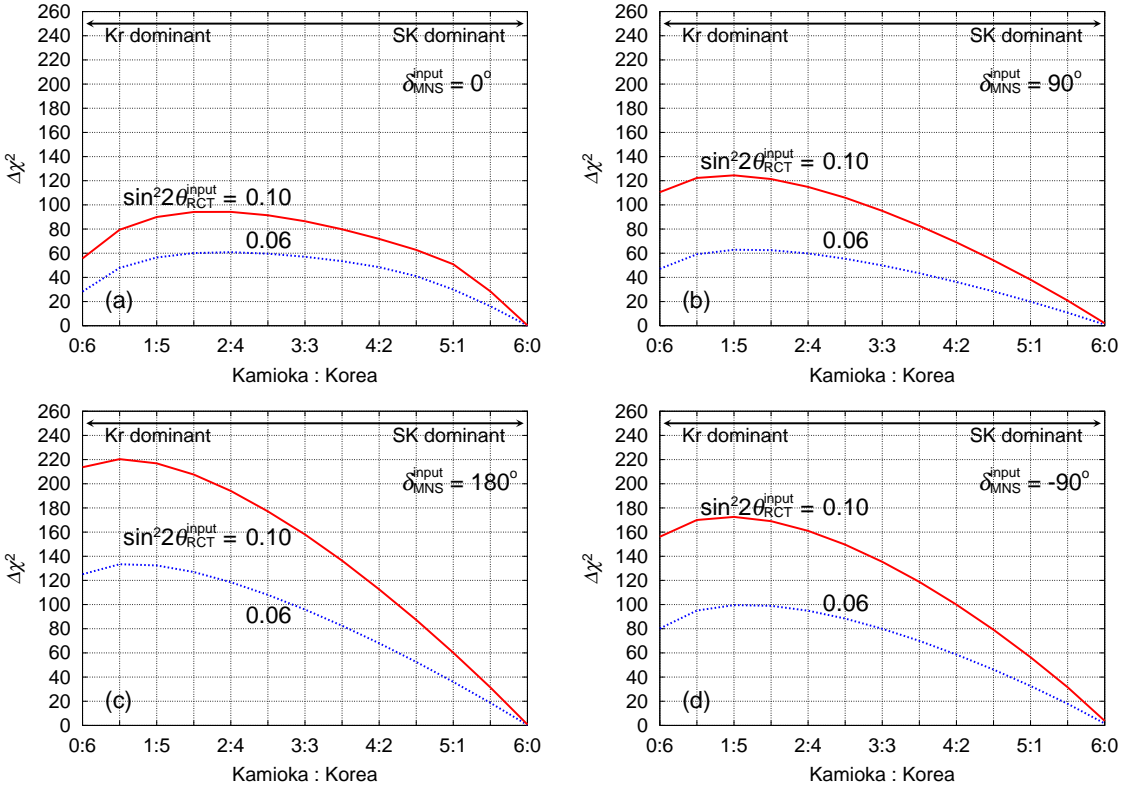


Figure 10: Optimal ratio of the fiducial volumes of two detectors, one at Kamioka ($L = 295$ km) and the other at $L = 1000$ km in Korea, for determining the neutrino mass hierarchy. The input data are calculated for the normal hierarchy at $m_3^2 - m_1^2 = 2.5 \times 10^{-3} \text{ eV}^2$ and the minimum $\Delta\chi^2$ of the fit with the wrong hierarchy is shown for $\sin^2 2\theta_{\text{RCT}}^{\text{input}} = 0.10$ (solid lines) and 0.06 (dotted lines) and for $\delta_{\text{MNS}}^{\text{input}} = 0^\circ$ (a), 90° (b), 180° (c), and 270° (d), when the sum of the fiducial volumes is fixed at 600 kt. The other parameters are same as those in Fig. 1 (d), and the results are calculated for 5×10^{21} POT.

the oscillation probabilities.

Our results are based upon a very simple treatment of the systematic errors where 3% overall errors are assigned for all the 10 normalization factors of eq. (31). We find that the significance of the mass hierarchy determination is not affected much even if we enlarge all the systematic errors to 10% except for the matter density uncertainties. This means that the errors of the T2KK experiment proposal in this paper are dominated by the statistical error. Therefore, if we make the detectors at Kamioka and/or Korea larger, or if the intensity of the J-PARC beam is stronger, the significance of the measurement will grow as proportional to the square root of the product of the volume, the intensity, and the exposure time. It is not so clear, however, what is the best volume ratio between the detector in Kamioka and that in Korea. We show in Fig. 10 the minimum $\Delta\chi^2$ as functions of the volume ratio of the near (Kamioka) and far (Korea) detectors while keeping the total volume at 600 kt for 5×10^{21} POT. We assume the normal hierarchy for the input and the inverted hierarchy in the fit. We examine 8 cases, for $\sin^2 2\theta_{\text{RCT}}^{\text{input}} = 0.1$ (solid lines) and $\sin^2 2\theta_{\text{RCT}}^{\text{input}} = 0.06$ (dotted lines), and for $\delta_{\text{MNS}}^{\text{input}} = 0^\circ$ (a), 90° (b), 180°

(c), and -90° (d). It is clearly seen from Fig. 10 that a 600 kt detector in Kamioka alone cannot resolve the mass hierarchy at all, because there is a little difference in $\nu_\mu \rightarrow \nu_e$ transition probability between the normal hierarchy and the inverted hierarchy. On the other hand, in the case of only a Korean detector with 600 kt, the minimum $\Delta\chi^2$ value is not much smaller than the best case. This is because the constraint of $\sin^2 2\theta_{\text{RCT}}$ from the future reactor neutrino experiment replaces the role of the near detector which measures the $\nu_\mu \rightarrow \nu_e$ transition at low energies where the matter effect is small. We find that the minimum $\Delta\chi^2$ value of 23.5 in Fig. 10(a) at the volume ratio of 1:5 ($\approx 22.5 : 100$) is about 4.5 times as large as the minimum $\Delta\chi^2$ value in Fig. 4(b), confirming the dominance of the statistical error in our analysis. If we request that the minimum $\Delta\chi^2$ should be at least 80% of its optimal value, then the near-to-far volume ratio should be between 0.5 : 5.5 and 2.5 : 3.5. More volumes should be given to the far detector than to the near detector.

It should also be noted that the capability of our T2KK setup to measure δ_{MNS} uniquely without invoking an anti-neutrino beam is advantages, because the anti-neutrino cross section on the matter is less than half of the neutrino cross section. The proposals that make use of anti-neutrino beams should suffer not only from smaller signal cross section but also from large background events.

Among the potentially serious background which we could not estimate in this paper are;

- possible miss-identification of NC π^0 production as ν_e CCQE events,
- possible miss-identification of soft π emission events as CCQE events.

Although the above uncertainties were found to be rather small at K2K experiments [32], we should expect them to be more serious at high energies. Dedicated studies of their effects on the neutrino-energy reconstruction efficiency are mandatory. In addition, careful studies including possible energy dependence of the flux and cross section uncertainties, and also the location dependence of the matter density, may be needed to justify the physics case of the T2KK proposal.

Acknowledgments

We thank our colleagues Y. Hayato, A.K. Ichikawa, T. Ishii, I. Kato, T. Kobayashi and T. Nakaya, from whom we learn about the K2K and T2K experiments. We are also grateful to Mayumi Aoki, Paul H. Frampton, Chung-Wook Kim, Soo-Bong Kim, and Yeongduk Kim, for useful discussions and comments. The work is supported in part by the Core University Program of JSPS. The numerical calculations were partly carried out on Altix3700 BX2 at YITP in Kyoto University.

References

- [1] The LSND Collaboration (A. Aguilar *et al.*), Phys. Rev. **D64**, 112007 (2001) [hep-ex/0104049].
- [2] M. Ambrosio *et al.* (MACRO Collaboration), Phys. Lett. **B566** 35 (2003) [hep-ex/0304037]; M. C. Sanchez *et al.* (Soudan 2 Collaboration), Phys. Rev. **D68**, 113004 (2003) [hep-ex/0307069]; Y. Ashie *et al.* (Super-Kamiokande Collaboration), Phys. Rev. **D71**, 112005 (2005) [hep-ex/0501064].

- [3] M. H. Ahn *et al.* (K2K collaboration) [hep-ex/0606032]
- [4] P. Adamson *et al.* (MINOS Collaboration), Phys. Rev. **D73**, 072002 (2006) [hep-ex/0512036].
- [5] M. B. Smy *et al.* (Super-Kamiokande Collaboration), Phys. Rev. **D69**, 011104 (2004) [hep-ex/0309011]; B. Aharmim *et al.* (SNO Collaboration), Phys. Rev. **C 72**, 055502 (2005) [nucl-ex/0502021].
- [6] T. Araki *et al.* (KamLAND Collaboration), Phys. Rev. Lett. **94**, 081801 (2005) [hep-ex/0406035].
- [7] M. Apollonio *et al.* Eur. Phys. J. **C27** 331 (2003) [hep-ex/0301017].
- [8] Y. Itow *et al.*, [hep-ex/0106019]. see also the JHF Neutrino Working Group's home page, <http://neutrino.kek.jp/jhfnu/>.
- [9] J-PARC home page, <http://j-parc.jp/>.
- [10] K. Hagiwara, Nucl. Phys. Proc. Suppl. **137**, 84 (2004) [hep-ph/0410229].
- [11] M. Ishituka, T. Kajita, H. Minakata, H. Nunokawa, Phys. Rev. **D72**, 033003 (2005) [hep-ph/0504026]
- [12] K. Hagiwara, N. Okamura, K. Senda, Phys. Lett. **B637** 266 (2006) [hep-ph/0504061].
- [13] P. Lipari, Phys. Rev. **D61**, 113004 (2000) [hep-ph/9903481]; M. Narayan, S. Uma Sankar, Phys. Rev. **D61**, 013003 (2000) [hep-ph/9904302]; V. Barger, S. Geer, R. Raja, K. Whisnant, Phys. Lett. **B485**, 379 (2000) [hep-ph/0004208].
- [14] V. Barger, D. Marfatia, K. Whisnant, Phys. Rev. **D65**, 073023 (2002) [hep-ph/0112119].
- [15] M. Aoki *et al.*, Phys. Rev. **D67**, 093004 (2003) [hep-ph/0112338].
- [16] O. Mena Requejo, S. Palomares-Ruiz, S. Pascoli, Phys. Rev. **D72**, 053002 (2005) [hep-ph/0504015]
- [17] Z. Maki, M. Nakagawa and S. Sakata, Prog. Theor. Phys. **28**, 870 (1962).
- [18] L. Wolfenstein, Phys. Rev. **D17**, 2369 (1978); R.R. Lewis, *ibid.* **21**, 663 (1980); V. Barger, S. Pakvasa, R.J.N. Phillips and K. Whisnant, *ibid.* **22**, 2718 (1980).
- [19] S.P. Mikheyev and A.Yu. Smirnov, Yad. Fiz. **42**, 1441 (1985) [Sov.J.Nucl.Phys.**42**, 913 (1986)]; Nuovo Cimento **C9**, 17 (1986).
- [20] K. Hagiwara and N. Okamura, Nucl. Phys. **B548**, 60 (1997).
- [21] G. L. Fogli, E. Lisi, A. Marrone and G. Scioscia, Phys. Rev. **D59**, 033001 (1999) [hep-ph/9808205]; G. L. Fogli, E. Lisi, A. Marrone, D. Montanino, A. Palazzo and A. M. Rotunno, Phys. Rev. **D69**, 017301 (2004) [hep-ph/0308055].

- [22] J. Arafune, M. Koike, J. Sato, Phys. Rev. **D56**, 3093 (1997) [hep-ph/9703351]; Erratum *ibid.* **D60**, 119905 (1999).
- [23] M. Koike, N. Okamura, M. Saito and T. Takeuchi, Phys. Rev. **D73**, 053010 (2006)[hep-ph/0510082].
- [24] The Double-CHOOZ Collaboration [hep-ex/0405032]. M. G. T. Lasserre,[hep-ex/0606025].
- [25] F. Suekane (for the KASKA Collaboration) [hep-ex/0407016].
- [26] T. Bolton, Nucl. Phys. Proc. Suppl. **149**, 166 (2005).
- [27] J. Cao, Nucl. Phys. Proc. Suppl. **155**, 229 (2006) [hep-ex/0509041].
- [28] S. B. Kim, talk presented in ‘Fourth Workshop on Future Low Energy Neutrino Experiments’, Angra dos Reis, RJ - Brazil (2005)
- [29] J. C. Anjos *et al.*, Nucl. Phys. Proc. Suppl. **155**, 231 (2006) [hep-ex/0511059].
- [30] D. S. Ayres *et al.* (NOvA Collaboration) [hep-ex/0503053].
- [31] A.K. Ichikawa, private communication; the flux datas for various off-axis angles are available this web page; <http://jnusrv01.kek.jp/~ichikawa/jhfnu/nubeam/655km>
- [32] K2K Collaboration (S. Nakayama *et al.*), Phys. Lett. **B619** 255 (2005) [hep-ex/0408134]